EFFECTS OF ZIRCONIA AND HYDROXYAPATITE NANOPARTICLES ON THE MECHANICAL PROPERTIES OF THE RESIN-BASED DENTAL COMPOSITES

A Thesis Submitted to
the Graduate School of Engineering and Sciences of
İzmir Institute of Technology
in Partial Fulfillment of the Requirements for the Degree of

MASTER OF SCIENCE

in Mechanical Engineering

by
Senagül TUNCA TAŞKIRAN

June 2023
İZMİR

We approve the thesis of **Senagül TUNCA TAŞKIRAN**

Examining Committee Members:

_____
Prof. Dr. Metin TANOĞLU
Department of Mechanical Engineering, İzmir Institute of Technology

_____
Prof. Dr. Ekrem ÖZDEMİR
Department of Chemical Engineering, İzmir Institute of Technology

_____
Assoc. Prof. Dr. Aylin ZİYLAN
Department of Metallurgical and Materials Engineering, Dokuz Eylül University

20 June 2023

_____
Prof. Dr. Metin TANOĞLU
Supervisor, Department of Mechanical
Engineering, İzmir Institute of Technology

_____   _____
Prof. Dr. M. İ. Can DEDE   **Prof. Dr. Mehtap EANES**
Head of the Department of Mechanical   Dean of the Graduate School
Engineering

ACKNOWLEDGEMENTS

ABSTRACT

EFFECTS OF ZIRCONIA AND HYDROXYAPATITE NANOPARTICLES ON THE MECHANICAL PROPERTIES OF THE RESIN-BASED DENTAL COMPOSITES

The majority of the population suffers from dental caries, one of the most common chronic diseases. Therefore, restoration of teeth is an urgent need. The materials used in restoration are composites prepared by adding inorganic components to the polymeric matrix. However, failure due to fractures and secondary caries is still the main problem. Therefore, studies are continuing to improve the mechanical properties and water sorption and solubility properties of the composite.

In this study, effects of zirconia, which improves the mechanical properties, and hydroxyapatite nanoparticles, which are the components of the tooth, on the mechanical properties of the composite were investigated. According to the literature, amounts of additives were determined as 1 and 2 wt.% for zirconia and 3 and 5 wt.% for hydroxyapatite. Nine different composites were prepared by mixing with hand spatulation method and mortar mill. The flexural strength and modulus, compressive strength, depth of cure, water sorption and solubility properties of the composites were investigated. Samples were characterized by using Scanning Electron Microscopy (SEM) and Fourier Transform Infrared Spectroscopy (FTIR).

Zirconia and HA particles significantly improved the flexural and compressive strength of the composites. The highest flexural strength was obtained in the sample containing 5 wt.% hydroxyapatite and 1 wt.% zirconia, with an increase of 58% compared to the control sample. The highest compressive strength was obtained in the sample containing 3 wt.% hydroxyapatite and 2 wt.% zirconia, with an increase of 22% compared to the control sample. Therefore, zirconia and HA nanoparticles have a synergistic effect.

ÖZET

ZİRKONYA VE HİDROKSİAPATİT NANOPARÇACIKLARININ REÇİNE ESASLI DİŞ KOMPOZİTLERİNİN MEKANİK ÖZELLİKLERİ ÜZERİNDEKİ ETKİLERİ

Nüfusun çoğunluğu, en yaygın kronik hastalıklardan biri olan diş çürüğü probleminden şikâyet etmektedir. Bu nedenle dişlerin restorasyonu acil bir ihtiyaçtır. Restoratif tedavide kullanılan malzemeler polimerik matrise inorganik bileşenlerin eklenmesi ile hazırlanan kompozitlerdir. Ancak klinik kullanımda kırık ve ikincil çürüklere bağlı başarısızlık hala reçine esaslı diş kompozitleri ile ilgili temel sorundur. Bu yüzden kompozitin mekanik özellikleri ile su emme ve çözünürlük özelliklerinin iyileştirilmesi için çalışmalar sürmektedir.

Bu tez çalışmasında; kompozitin mekanik özelliklerini iyileştirmesi ile bilinen zirkonya ve dişin yapısında bulunan hidroksiapatit nanoparçacıklarının kompozitin mekanik özellikleri üzerindeki etkileri incelenmiştir. Literatüre göre zirkonya için ağ.%1 ve 2 ve hidroksiapatit için ağ.% 3 ve 5 ve olmak üzere farklı ilave miktarları belirlenmiştir. El spatulası yöntemi ve havanlı öğütücü yardımı ile karıştırılarak dokuz farklı kompozit hazırlanmıştır. Hazırlanan kompozitlerin eğme mukavemeti ve modülü, basma mukavemeti, kürlenme derinliği ve su emilimi ve çözünürlük özellikleri araştırılmıştır. Numuneler, taramalı elektron mikroskobu (SEM) ve Fourier Dönüşümlü Kızılötesi Spektroskopisi (FTIR) kullanılarak karakterize edilmiştir.

Zirkonya ve HA nanoparçacıkları, kompozitlerin eğilme ve basınç dayanımında önemli bir gelişme göstermiştir. En yüksek eğilme mukavemeti ağ.%5 hidroksiapatit ve ağ.%1 zirkonya içeren numunede elde edilmiş ve kontrol numunesine göre %58 artış sağlanmıştır. En yüksek basınç dayanımı ise ağ.%3 hidroksiapatit ve ağ.%2 zirkonya içeren numunede elde edilmiş olup, REF numunesine göre %22 artış sağlanmıştır. Zirkonya ve HA nanoparçacıklarının sinerjik bir etkiye sahip olduğu söylenebilir.

TABLE OF CONTENTS

LIST OF FIGURES

LIST OF TABLES

CHAPTER 1

INTRODUCTION

Teeth are very important in terms of health, aesthetics, and quality of life for humans. It is the only part of the human body that is exposed to mechanical stress, temperature, and pH changes. The teeth allow food to be digested by chewing and are the beginning of the digestive system. However, food residues may remain in the oral cavity and cause the formation of bacteria. This leads to plaque formation and ultimately tooth caries (Jin Chun, Yeon Kim, and Yeop Lee 2016). Most people suffer from tooth caries problem which is one of the most common chronic diseases in the world (Zhou et al. 2019). These caries can lead to defects in dental functions. While the human body can regenerate damaged parts in an incredible way, the same situation is not valid for teeth. Therefore, restoration of teeth is an urgent need. Dental restorative materials are used in clinical treatment and reconstruction to restore the function of teeth. With these materials, the cavities in the enamel and dentin caused by caries are filled and the teeth can regain their normal shape and functions (Hu et al. 2019).

Amalgam was the most widely used restorative material for many years in the past. However, controversy has been started because it contains mercury, which is known as toxic. In addition, aesthetic concerns have become more prominent. For this reason, the necessity to turn to an alternative material has emerged. As a result, resin-based composites have been noticed and overcome the disadvantages of amalgam. However, there are still some difficulties regarding these materials. Although these systems have undergone some structural changes over the years, developments continue today (Najafi et al. 2017).

Resin-based dental composites have three main components including the resin matrix, the reinforcing phase dispersed in this resin matrix, and the silane coupling agent used to achieve a good chemical bond between the resin matrix and the reinforcement. Methacrylate-based resins are preferred as matrices due to their biocompatibility, easy formability, and mechanical and aesthetic properties. As the reinforcement phase, various ceramic-based inorganic filler particles are preferred. The amount of filler in current commercial composites varies between 70-80 wt.%. These composites also contain

ingredients such as initiators and accelerators for the kinetics of the polymerization reaction. Although resin-based dental composites are divided into three groups according to their curing mechanism, the polymerization of dental composites used today is carried out using visible light (Miletic 2018).

The main problem with resin-based dental composites is failure due to fracture and secondary caries, which compromises long-term durability in clinical use (Zhou et al. 2019). In order to overcome these problems, the mechanical properties and water sorption and solubility properties of the composite must be improved. Many studies have been carried out with combinations of different monomer and inorganic filler particles to achieve it. In particular, it is reported that the type and amount of inorganic particles used have a critical effect on the mechanical properties of the composite (Miao et al. 2012).

Silica and borosilicate glasses are used as inorganic filler particles in almost all composites. These are the most widely used particle types because they give positive results with silane coupling agents. Zirconia particles, which are known to show biocompatibility, improve the mechanical properties of the composite and provide aesthetic properties. They also have an antibacterial effect that can prevent secondary caries formation. However, it has disadvantages such as increased water sorption and solubility and decreased depth of cure (Bapat et al. 2022). Zirconia has been suggested to be suitable for dental restorations and is already used alongside silica in available commercial composites (X. Y. Zhang et al. 2014).

In addition to these inorganic particles, hydroxyapatite which is a calcium phosphate-based ceramic and is present in the structure of the tooth has recently been investigated. Hydroxyapatite is considered as a good candidate as fillers thanks to its similarity with teeth and bones and its biological and mechanical properties. When it is used in dental composites, it provides high bioactivity by preventing demineralization and remineralization by releasing calcium and phosphate (Aydınoğlu et al. 2022). It reduces the formation of secondary caries. Its low fracture toughness limits its use alone as a filler. For this reason, it is recommended to be used with different inorganic filler particles, especially silica (Razali et al. 2018).

There is no study in which zirconia and hydroxyapatite particles are used together and their effects on the physical properties of the composite are examined. It is not known whether the two particle types counteract each other's disadvantages and together have a synergistic effect on the physical properties of the composite.

The aim of this study is to examine the single and cross effects of zirconia and hydroxyapatite nanoparticles on the mechanical properties, water sorption and solubility properties of the composite. It is expected to improve the mechanical properties of the composite, as well as water sorption and solubility properties. Within the scope of this study, 3^2 full factorial experimental design was used. Two particle types, zirconia, and hydroxyapatite, were determined as factors, and three different particle amounts were selected as levels for both factors. The amount of particles to be added was determined according to the literature. While 3 and 5 wt.% were preferred for hydroxyapatite; 1 and 2 wt.% were preferred for zirconia nanoparticles. According to this experimental design, nine different samples were prepared. The flexural strength and flexural modulus, compressive strength, depth of cure, and water sorption and solubility properties of these composites were investigated and compared. Samples were characterized by using Scanning Electron Microscopy (SEM) and Fourier Transform Infrared Spectroscopy (FTIR).

.

CHAPTER 2

RESIN-BASED DENTAL RESTORATIVE COMPOSITES

2.1   Structure of a Tooth

Human teeth have a more complex structure and better mechanical properties than synthetic restorative materials. They can be divided into three primary parts including the crown, the neck, and the root. The crown is the visible portion of the tooth. The neck is the area located at the gum line, between the crown and the root. The root serves as the anchor of the tooth and extends into the jawbone. The mechanical properties of teeth are determined by their structure and composition. The structure of natural teeth consists of enamel, dentin, cementum, and dental pulp. The first three of these constitute hard tissue and are characterized by unique mechanical properties (Y. R. Zhang et al. 2014). The structure of the teeth is presented in Figure 2.1.
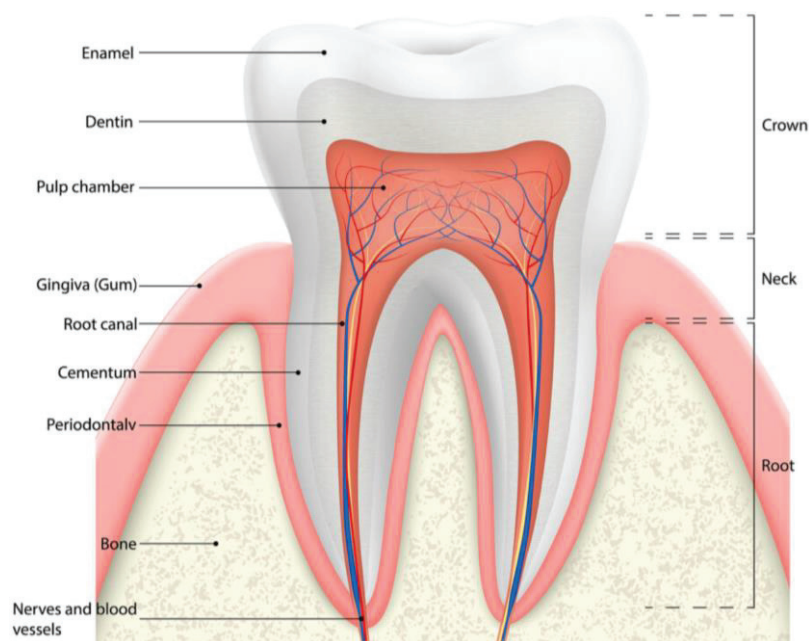
Figure 2.1 Cross-section of an adult human tooth (Source: Y. R. Zhang et al. 2014)

Enamel is the visible, white, and shiny outer surface of the tooth. It represents the hardest tissue in the body. It consists almost entirely of tightly arranged mineral-type hydroxyapatite (a crystalline calcium phosphate) in a protein matrix structure, in addition to a few percent Water (Neuse and Mizrahi 2003). Dentin is the main component of the tooth interior and lies beneath the enamel and cementum. Its structure is more like bone. It surrounds the pulp chamber and root canals. It contains less mineralized phase, therefore it is softer. Dentin is composed of small tubules that radiate from the pulp to the enamel margin throughout its structure. Therefore, it can be said that it is a living tissue. Dentin contains rich collagen fibers (Y. R. Zhang et al. 2014). The composition of enamel and dentin layers in the tooth is given in Table 2.1.

Table 2.1 Composition of enamel and dentin layers (Source: Y. R. Zhang et al. 2014)

Component	Content (wt.%)	
	Enamel	Dentin
Mineral matter (mostly hydroxyapatite)	97	69
Organic matter (mostly proteinaceous)	1	20
Water	2	11

The pulp is the central chamber of the tooth. It is a soft tissue that contains blood vessels that provide nourishment to the tooth and nerves that allow the tooth to sense heat and cold. The dentin under the gum is covered with a thin layer of cementum. Cementum has a structure similar to bone tissue, but its hardness is lower than dentin. Moreover, the pulp contains lymph vessels, which play a role in transporting white blood cells to the tooth to aid in combating bacterial infections (Y. R. Zhang et al. 2014).

Teeth are divided into two groups as anterior and posterior. The incisor and canines are anterior, while the premolar and molar are posterior. This classification is shown in Figure 2.2. The morphology of the occlusal surface varies according to the type of tooth. Occlusal means chewing surface. It is the part of the teeth that is in contact with the opposing teeth during biting and chewing.
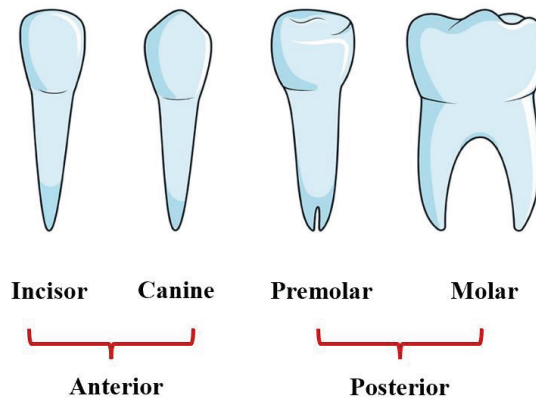
Figure 2.2 Classification of the types of tooth

The incisors are the front teeth located top and bottom of the mouth. The occlusal surface of the incisors has a chisel-like shape, which allows them to cut and shear food efficiently. Canines are sharp-pointed teeth and get their name from their similarity to dog teeth. This allows the teeth to tear and pierce food. Premolars and molars have a more complex occlusal surface. Typically, they have two or more cusps that interlock with opposing teeth during occlusion. They allow us to grind or crush food before swallowing it.

In general, flexural strength is more critical for anterior teeth as they are subject to bending forces during biting and cutting actions. Compressive strength is more important for posterior teeth as they are exposed to compressive forces during grinding and crushing actions. However, both flexural and compressive strength are necessary for all teeth, as different forces can be experienced depending on the specific situation and the type of food consumed (Jin Chun, Yeon Kim, and Yeop Lee 2016). Some mechanical properties of tooth structure are given in Table 2.2.

Table 2.2 Selected mechanical properties of tooth structure Y. R. Zhang et al. 2014)

Property	Enamel	Dentin
Compressive strength (MPa)	100-380	250-350
Modulus of elasticity (GPa)	10-80	20-50
Vickers hardness number	350	60

2.2 Resin-Based Dental Composites

Resin-based dental restorative composites consist of a polymerizable resin and various fillers that are evenly dispersed in the resin. In the mid-1960s, resin-based composite materials began to be used as restorative materials. Thus, problems caused by amalgam such as corrosion and low adhesion, especially toxicity and aesthetic appearance were prevented. However, they also have drawbacks, including polymerization shrinkage, water sorption and solubility, and low wear resistance (Miao et al. 2012). These are critical for the life of the restorative material. Therefore, researchers have conducted numerous studies to enhance the clinical performance of resin-based dental composites, exploring different matrix materials and examining the types, sizes, and quantities of the fillers (Yushau, Almofeez, and Bozkurt 2020).

2.3 Components of Resin-Based Dental Composites

Resin-based dental composites have three main components. These components are (i) resin matrix (organic phase), (ii) filler particles dispersed in this resin matrix (inorganic phase), and (iii) silane coupling agent used to achieve a good chemical bonding between the resin matrix and filler particles. These composites also contain ingredients such as initiators and accelerators for the kinetics of the polymerization reaction, inhibitors to prevent undesirable polymerization under storage conditions, and pigments to achieve a color compatible with teeth (Miletic 2018).

2.3.1 Organic Phase

In resin-based dental composites, methacrylate-based resins are used as matrix material. Bowen developed a high molecular weight monomer called Bis-GMA (bisphenol A glycidyl methacrylate) in 1962 by reacting bisphenol-A and glycidyl methacrylate. Bis-GMA is the most commonly used resin monomer. However, it is an

extremely viscous material (η = 1200 Pa.s) because of the hydrogen bonding between the monomer molecules and the hydroxyl groups. This will result in an extremely hard composite for clinical use, even with a small amount of filler. Therefore, Bis-GMA is mixed with lower viscosity comonomers which are called diluent. For this, TEGDMA (triethylene glycol dimethacrylate) is preferred. TEGDMA (η = 0.006 Pa.s) is a significant factor in controlling the viscosity of resin-based dental composites (Najafi et al. 2017).

Bis-GMA is controversial because BPA (bisphenol A) is used during its synthesis. Traces of BPA may remain in the composite after production. Small amounts of BPA may be released because of the hydrolysis caused by saliva enzymes. Biological risk still is a controversial issue, although it is unlikely. For this reason, UDMA (urethane dimethacrylate) has been introduced. UDMA has a lower molecular weight compared to Bis-GMA. When it is used instead of Bis-GMA, less viscous resin mixtures were obtained. Thus, the need for diluent has been reduced. In addition, one of the monomers that can be replaced with TEGDMA is Bis-EMA (ethoxylated bisphenol A glycol dimethacrylate) since TEGDMA has a relatively higher shrinkage and slightly hydrophilic nature (Miletic 2018). Bis-EMA is a high molecular weight and low viscosity resin obtained by removing hydroxyl groups from Bis-GMA monomer. It has been reported that it has advantages such as low shrinkage and stickiness. The properties and chemical structures of these monomers are given in Table 2.3 and Figure 2.3, respectively.

Table 2.3 Properties of monomers widely used in dental composites (Source: Barszczewska-Rybarek 2019)

Monomers	Chemical Nomenclature	Molecular Weight (g/mol)	Viscosity (Pa.s)	Molecular Formula
Bis-GMA	bisphenol A glycidyl methacrylate	512	1200	$C_{29}H_{36}O_8$
UDMA	urethane dimethacrylate	470	23	$C_{23}H_{38}N_2O_8$
TEGDMA	triethylene glycol dimethacrylate	286	0.01	$C_{14}H_{22}O_6$
Bis-EMA	ethoxylated bisphenol A dimethacrylate	540	0.9	$C_{39}H_{44}O_8$
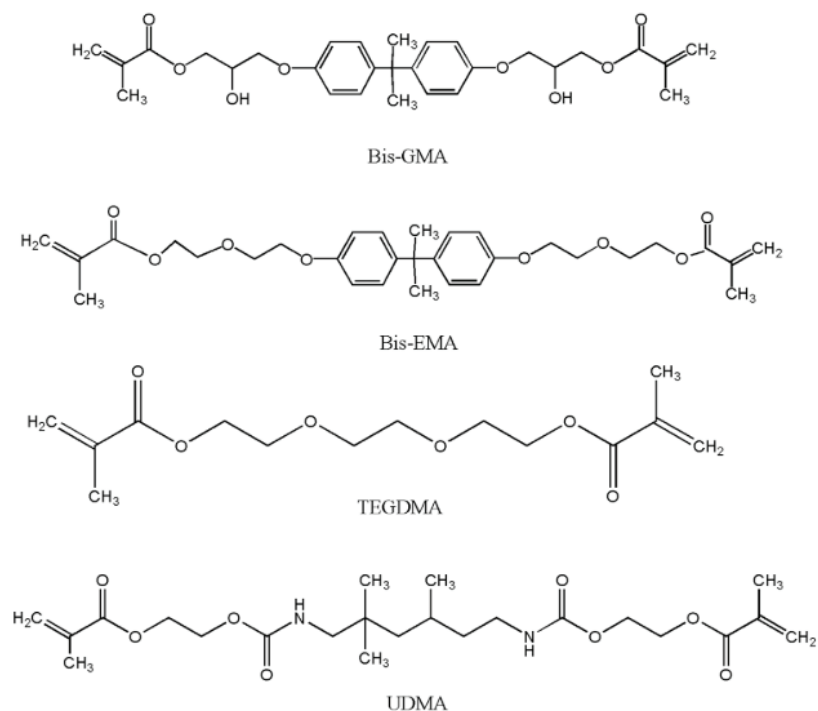
Figure 2.3 Chemical structures of widely used monomers (Source: Pratap et al. 2019)

2.3.2 Inorganic Phase

The properties of a dental composite are primarily determined by the type, concentration, size, and size distribution of the fillers. Inorganic filler particles are the reinforcement phase in the composite. These particles increase the modulus of elasticity, provide resistance to abrasion, improve fracture toughness, and give the practitioner the ability to form the material before curing. In addition, fillers can reduce water sorption and polymerization shrinkage, add radio-opacity and increase aesthetic properties. However, fillers must be loaded in optimal amounts and distributed homogeneously in the resin matrix to obtain these property improvements (Miletic 2018).

Inorganic fillers can be divided into two groups including conventional and modern. Conventional fillers include macro and micro fillers, while modern ones are hybrid and nanofillers. Historically, the first fillers used were large micron-sized particles larger than 10 μm. A reduction in average particle size should have been provided as improved mechanical properties and higher filler loading has been needed. As a result, finer micron-sized and then nano-sized particles have been introduced (Chaughule 2018).

The first commercial nano-filled dental composite, Filtek Supreme by 3M ESPE, was introduced to the market in 2002. The historical evaluation of the particles in terms of size is given in Figure 2.4.

Macrofilled	Microfilled	Microhybrid
10-50 μm	0.1-10 μm	average 0.6 μm
1960-1970	1970-1980	1980-1990
Nanofilled (agglomerate)	Nanofilled (discrete)	Nanohybrid
20–100 nm	1–100 nm	average < 0.1 μm
	2000	Mid-2000's
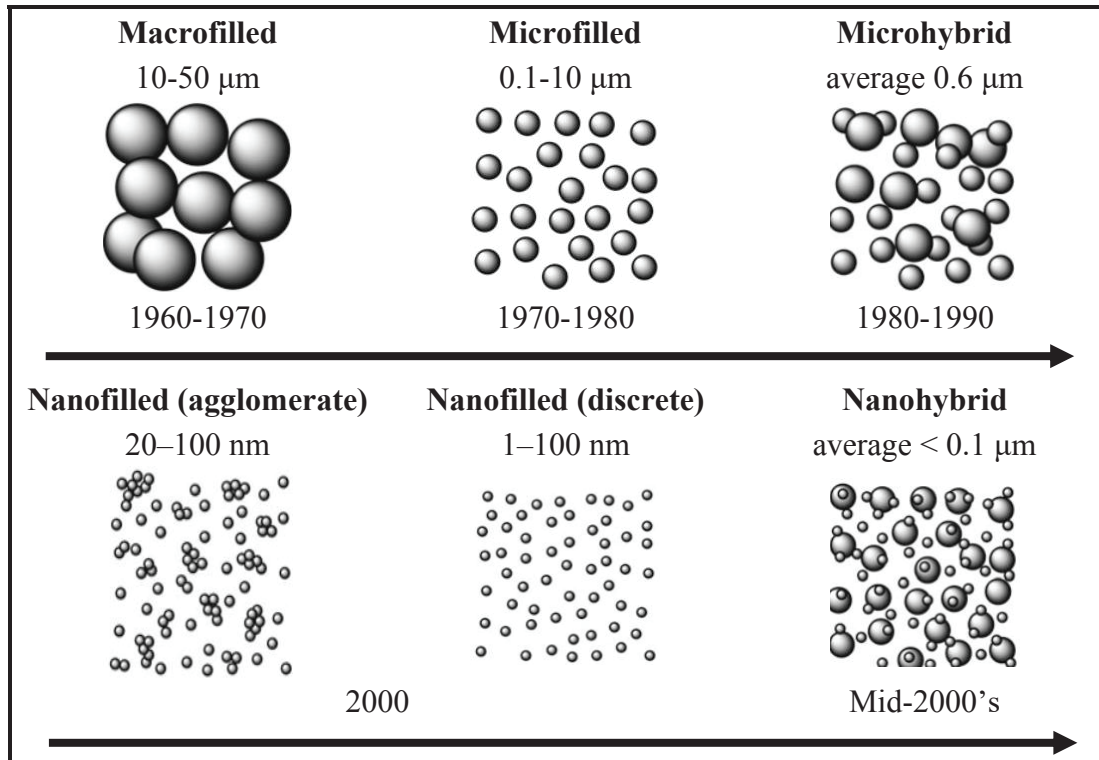
Figure 2.4 The historical evaluation of the particles in terms of size (Source: Chaughule 2018)

Nanofillers can reduce the space between the filler particles by enabling a greater amount of filler to be loaded into the composite material, resulting in improved physical properties and a smoother surface finish. The amount of the nanofillers can theoretically be up to 90-95% by weight. However, there is a relationship between the filler loading and the surface area of the filler particles. As the surface area of the particles increases with the increasing amount of filler, the wettability of the fillers is adversely affected. Therefore, the amount of nanofillers is practically lower (Khurshid et al. 2015). The amount of filler in current commercial composites varies between 70-80 wt.%.

Nanohybrid composites contain both large particles (0.4-5 μm) and nano-sized particles. It can be difficult to distinguish nanohybrid from microhydrid composites and

they tend to have similar flexural strength and modulus of elasticity. The difference between them can be thought as the average particle size (Jack L. Ferracane 2011).

Commonly used fillers include oxides and types of glass. Silicon dioxide or silica (SiO_2), which is the first filler material used in these composites, is considered as the foundation for other glass fillers composed of different silicate compounds (McCabe and Walls 1969). Many metal oxides such as alumina (Al_2O_3), zirconia (ZrO_2), titanium dioxide (TiO_2), and zinc oxide (ZnO) have also been studied in addition to silica. Most commercial composites manufactured by 3M ESPE contain significant amounts of zirconia. Alkaline silicate glasses contain many different filler compositions. They consist mainly of silica. However, alkali oxides such as barium oxide (BaO) and strontium oxide (SrO) are also integrated into the silica network. The hardness of these materials is 5 Mohs and it is lower compared to silica, which is 7 on the Mohs scale. They offer an advantage in terms of X-ray radio-opacity due to the heavier integrated elements. This eliminates the need for additional radio-opacity agents, such as ytterbium or yttrium fluoride. The filler types and their chemical formulation is given in Table 2.4.

Table 2.4 Filler types and their chemical formulations (Source: Habib et al. 2016)

Filler Type	Example	Chemical Formulation
Oxides	silica, zirconia, alumina	M_xO_y
Biomimetic filler	hydroxyapatite	$Ca_5(PO_4)_3OH$
Alkaline silicate glass	barium glass, strontium glass	$M_xO_ySiO_2$
M=metal x=1,2 y=2,3		

2.3.2.1 Silica (SiO_2)

Silica fillers were originally produced with a top-down approach by grinding quartz. As a result of this process, coarse and irregularly shaped particles were obtained. These particles showed high flexural strength and modulus values. Despite this, the size and shape of the particles caused issues in the final material, such as high roughness and low wear resistance. Therefore, bottom-up approaches including solution particle synthesis and pyrogenic particle synthesis are currently preferred.

The refractive index of silica is 1.46. This value is below the traditional Bis-GMA/TEGDMA resin mixture. Therefore, when it is used with these resins, it becomes more opaque compared to other fillers. Silica is widely used in dental composites. One of the reasons for this can be the positive result of silica particles with silane coupling agents (Habib et al. 2016).

2.3.2.1.1 Fumed Silica

Silica pyrogenesis is a process in which silicon tetrachloride or quartz sand is superheated. These silica particles are called pyrogenic or fumed silica. Fumed silica is produced through a vapor-phase hydrolysis process of silicon tetrachlorides in a hydrogen-oxygen flame, as illustrated in Figure 2.5. The resulting process generates silicon dioxide molecules that condense to form particles. These particles collide, attach, and sinter together to form a three-dimensional branched-chain aggregate. With this method, nano-sized particles and particle aggregates are created. Very small particles with large surface areas are obtained in the range of 5-50 nm (Miao et al. 2012). They have a higher purity compared to others. However, high energy requirements and harsh reaction conditions pose constraints in terms of the environment.
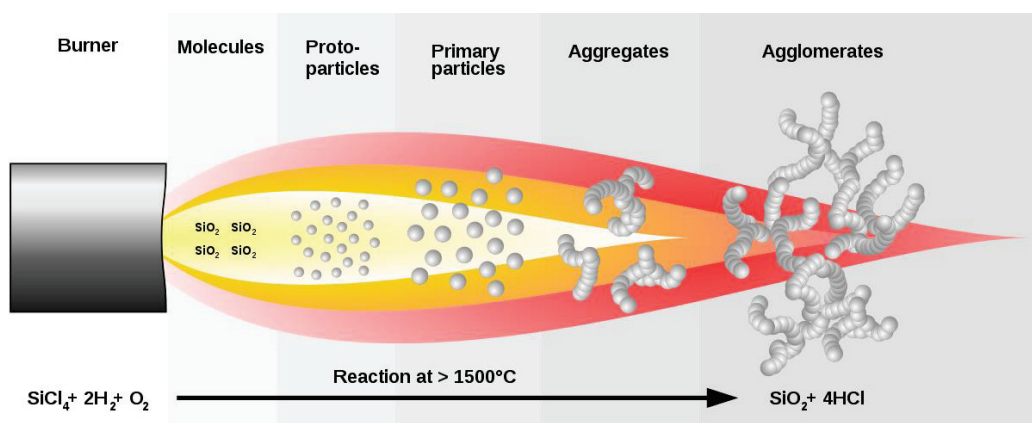
Figure 2.5 Schematic representation of silica pyrogenesis

Fumed silica is commonly used as a filler in resin-based dental composites, but the amount of particles added is very limited due to the enormous surface area of the particles. It allows them to interact with and adsorb a large amount of liquid including the resin where it is added. When fumed silica is added into a resin, it forms a network of aggregated particles that can trap and hold the liquid resin within its structure. This results in an increase in the viscosity of the resin, making it thicker and more difficult to flow (Hyde et al. 2016). Because silanol groups exist on the particle surface, fumed silica prepared using the pyrogenesis is hydrophilic and, therefore, has high surface energy. This makes it difficult to disperse in the resin without surface modification. Surface modification of silica can be achieved by grafting functional groups to the silica surface. In these processes, a hydrophilic surface with high surface energy transforms into a hydrophobic nature with low surface energy (Miao et al. 2012). Khaje & Jamshidi reported that it is not possible to wet more than 20 wt% of the modified particles in the resin because of the high specific surface area of the particles (Khaje and Jamshidi 2015).

Fumed silica can control the rheological properties of the composites. The addition of fumed silica can also improve the handling properties of dental composites by reducing the flow and stickiness of the material. It provides greater control and precision during the restoration process. It is important to carefully balance the amount of fumed silica added to the resin to avoid creating a material that is too thick and difficult to manipulate (Byrne 1984).

2.3.2.1.2 Colloidal Silica

The solution synthesis method is also called the "Stöber process" and it is the most widely used method. It produces particles with a spherical shape and uniform distribution. This method can produce particles ranging in size from 5 nm to several microns. The spherical particle shape provides high strength and also a lower surface roughness compared to ground quartz (Habib et al. 2016). Satterthwaite et al. reported that the use of nanosized and spherical-shaped particles in the composite results in lower polymerization shrinkage than that of irregularly shaped particles (Kaleem, Satterthwaite, and Watts 2009). It can be said that colloidal silica is a type of filler found in all commercial composites.

2.3.2.2 Zirconia (ZrO₂)

Zirconia has been used in biomedical applications since the 1960s. It has advanced mechanical properties, high fracture toughness, high chemical stability, high hardness, and excellent corrosion resistance. It also exhibits superior biocompatibility. Therefore, it has a wide application area today (Rao et al. 2019). It has been reported that zirconia provides an excellent color match with natural teeth. Considering its aesthetic properties as well as other properties, it is suitable for dental restorations (X. Y. Zhang et al. 2014).

Recent studies have shown that the addition of zirconia nanoparticles can significantly improve the mechanical properties of the materials (Bapat et al. 2022). Badr has compared the mechanical properties of resin-based dental composites with different concentrations (1, 3, 5, 7, and 10 wt.%) of zirconia nanoparticles. The addition of zirconia nanoparticles at 1 wt.% provided improved flexural strength, but at higher concentrations, it started to decrease (Al Badr 2018). Amdjadi et al. also investigated the effect of zirconia nanoclusters on the compressive strength of a dental composite and it was found that the compressive strength increased in correlation with the volume percentage of zirconia (Amdjadi et al. 2017). Zirconia nanoparticles not only increase the mechanical properties of dental composites, but also have an antibacterial effect that can prevent secondary caries formation, which is one of the main problems for these composites. However, it has disadvantages such as increased water sorption and solubility and decreased depth of cure because of its relatively high refractive index (Bapat et al. 2022). Wang et al. have successfully modified zirconia particles with γ-MPS and reported that it increased light transmission into deep layers of the composite due to a slight decrease in the refractive index (Wang et al. 2020).

Chan et al. reported that the addition of zirconia nanoparticles improved the fracture toughness of dental composites. The reason for this has been shown as the deflection of the crack propagation by the particles around the zirconia nanoparticles and along the matrix/particle interface. In the case of good matrix/particle interface bond strength, composites that are more resistant to fracture are obtained due to the high fracture toughness of zirconia nanoparticles (Chan et al. 2009).

Radio-opacity allows resin-based dental composites to be easily distinguished from surrounding tooth structures and facilitates the diagnosis of secondary caries. For this, a filler containing high atomic number elements should be used. Although Ba (56)

is generally preferred, Zr (40) is also used. Because of all these properties, it is widely preferred alongside silica in most existing commercial dental composites (Wang et al. 2020).

2.3.2.3 Hydroxyapatite

Hydroxyapatite (HA) is a calcium phosphate-based ceramic and its formulation is $Ca_5(PO_4)_3(OH)$. It is the main component of tooth structure. Nearly 96 wt.% of enamel and 70 wt.% of dentin consist of HA. It is considered as a good candidate as fillers thanks to its similarity with teeth and bones and biological and mechanical properties (Kantharia et al. 2014).

Almost 50-70% of restorations fail due to secondary caries formation caused by plaque-causing bacteria such as streptococcus mutans (S.Mutants), streptococcus aeurus (S.Aeurus), and lactobacilli. Therefore, it is of great importance to improve the natural tissue by preventing the formation of biofilms. It is reported that HA inhibits biofilm formation. When it is used in dental composites, it provides remineralization by releasing calcium and phosphate and high bioactivity by preventing demineralization. It is reported that HA reduces the formation of secondary caries, which is one of the main problems of resin-based dental composites (Aydınoğlu et al. 2022).

Different HA fillers such as spherical or whisker have been used in dental composites in the literature. Lezaja et al. have investigated the mechanical properties of dental composites which they prepared using HA spherical particles and whiskers. While HA spheres provided a 16% improvement in flexural and compressive strength, HA whiskers had a detrimental effect on the mechanical properties of the composite (Lezaja et al. 2013). Elfakhri et al. have reported that despite the surface modification, fillers with high aspect ratios were not distributed homogeneously due to unfavorable filler-matrix interface properties and reduced strength of the composites (Elfakhri et al. 2022). Chen et al. have prepared dental composites containing silica and HA. Different concentrations including 2, 3, 5, 7, and 10 wt.% of HA were added to the composites with a total filler content of 60 wt.%, respectively. While the highest flexural strength was obtained at 3 wt.%, further additions negatively affected the mechanical properties. The reason for this

is that the particles agglomerate with the increasing HA ratio and cannot strengthen the composite efficiently (L. Chen et al. 2011).

In addition to all these advantages, it is important that HA added composites meet the requirements of ISO 4049 standard. However, its low fracture toughness limits its use alone as a filler. For this reason, it is recommended to be used with different inorganic filler particles, especially silica (Razali et al. 2018). Liu et al. have evaluated the single effect of HA particles on dental composites. They reported that dental composites containing only HA particles as fillers were found to be unsuitable for practical applications because of their extremely high water sorption and solubility (Liu, Sun, et al. 2014).

Santos et al. have incorporated HA fillers, untreated and treated with silane, into the Bis-GMA resin. Silane treated HA particles provided better contact with the resin matrix. They also reported that water sorption decreased with the addition of silane treated HA (Santos et al. 2002).

Behiri et al. have reported that they achieved successful results in their study by adding HA filler treated with 3-methacryloxypropyltrimethoxysilane (γ-MPS) to a polymethylmethacrylate-based bone cement. Labella et al. also reported that the silanization of HA filler with γ-MPS had a net enhancing effect on the flexural strength of the resin-based dental composites (Labella, Braden, and Debt 1994).

2.3.2.4 Barium Glass

Resin-based dental composites are available in various shades and translucencies to ensure that the color of the composite is compatible with adjacent teeth, improve the aesthetic appearance of the restoration, and enable the photopolymerization to reach a significant depth (a few millimeters) in limited exposure times. The darker and more opaque shades in composites hinder sufficient light transmission, which reduces their depth of cure (El-Banna, Sherief, and Fawzy 2019). That's why, more translucent, "enamel" shades of composites should be obtained.

The depth of light penetration is determined by the ability of the light to reach the deep layers of the resin-based composites. However, there will be a loss of light due to refractions with depth. Therefore, the fillers used are critical in terms of light

transmittance of the composite in the visible range. The size and amount of the filler and refractive index between fillers and matrix are parameters that affect the optical properties of a dental composite.

Translucency is increased by reducing the filler content and the filler size. Nanofillers are in the size range of 10-40 nm. It is smaller than the wavelength of visible light (400-800 nm) (Jack L. Ferracane 2011). This situation decreases scattering which allows more photons to penetrate into deeper layers. Thus, highly transparent resin composites that increase light transmittance can be developed. Despite these advances, modern composites still fail to achieve the optical properties of natural enamel.

The law of refraction describes the deviation of light from its original direction at an interface due to the difference in refractive index between the two materials. An interface occurs between each filler particle and the resin. When the refractive index of the filler particles is similar to that of the resin matrix, it is expected that the light transmission and depth of cure will increase. The refractive index of polymers increases with increasing resin crosslink density. Therefore, the refractive index of the filler particles should be as close as possible to that of the cured copolymer mixture. Translucency increases in most existing commercial resin composites as polymerization progresses (Miletic 2018).

Silicate particles containing BaO generally exhibit higher refractive indices compared to silica, making them more similar to that of traditional resin matrix mixtures. They were used to set the refractive index of the other particles used from 1.46 to 1.55 (refractive index of the resin). This enables more transparent composites to be obtained. Despite their lower particle hardness, these materials have mechanical properties including abrasion resistance, strength, and modulus that are comparable to silica. They exhibit superior optical properties, making them a preferred choice for commercial materials (Habib et al. 2016). In the literature, the amount of Ba glass particles varies between 25-75 wt.% (Al Badr 2018; Hambire and Tripathi 2014). Refractive indices of the monomers and inorganic fillers are given in Table 2.5.

Table 2.5 Refractive indices of the monomers and inorganic fillers (Source: Habib et al. 2016; Miletic 2018; Pratap et al. 2019)

Resin Monomers	Refractive Index
Bis-GMA	1.55
UDMA	1.49
TEGDMA	1.46
Bis-EMA	1.49
Resin Mixtures	**Refractive Index**
Bis-GMA/TEGDMA 70/30	1.52→1.55[a]
Bis-GMA/TEGDMA 50/50	1.54[a]
Inorganic Fillers	**Refractive Index**
Silica	1.46
Zirconia	2.16
Hydroxyapatite	1.64
Barium borosilicate glass	1.55

[a] Refractive index after the polymerization

2.3.3 Initiator-Accelerator

The monomers have C=C (carbon double bond) in their chemical structure before the polymerization. During polymerization, these double bonds open and the monomers begin to form bonds with each other. In this way, polymer chains are formed. Polymerization begins with the formation of free radicals. Reactive substances called initiators and accelerators are required for the formation of free radicals. There are weak bonds in these substances that can be broken down by chemical or physical effects and provides the formation of free radicals. Radicals react with monomers having unsaturated double bonds. The free electron is added to the end of the chain and activates the monomer electron. Thus, the activated monomer is added to the other monomer and activates the next monomer. This chain reaction continues until all free radicals are bonded. Resin-based dental composites can be divided into three groups, based on their initiation system or curing mechanism including chemically-cured, light-cured or, dual-cured (Kwon et al. 2012).

For photopolymerization of the light-cured composites, LEDs with a wavelength of 450-490 nm are currently preferred due to their superior efficiency compared to

previous technologies (Santini 2010). The most widely used photoinitiator in light-cured resin composites is camphorquinone (CQ) thanks to its wide absorption range of 400 to 500 nm. Although CQ initiator systems are accepted, its yellowish color can negatively affect the color of the composite. As alternatives to CQ, phenyl-propanedione (PPD) and diphenyl (2,4,6-trimethylbenzoyl) phosphine oxide (TPO) can be used as photoinitiators. Since TPO and PPD are white in color, they eliminate the undesirable yellow color effect of CQ. In addition, there is another photoinitiator called Ivocerin™. It is a germanium-based photoinitiator and stands between CQ and TPO. (Cramer, Stansbury, and Bowman 2011). However, CQ is still the most common initiator because its absorption range is closest to the emission spectrum of the LEDs as seen in Figure 2.6 (Porto et al. 2010).
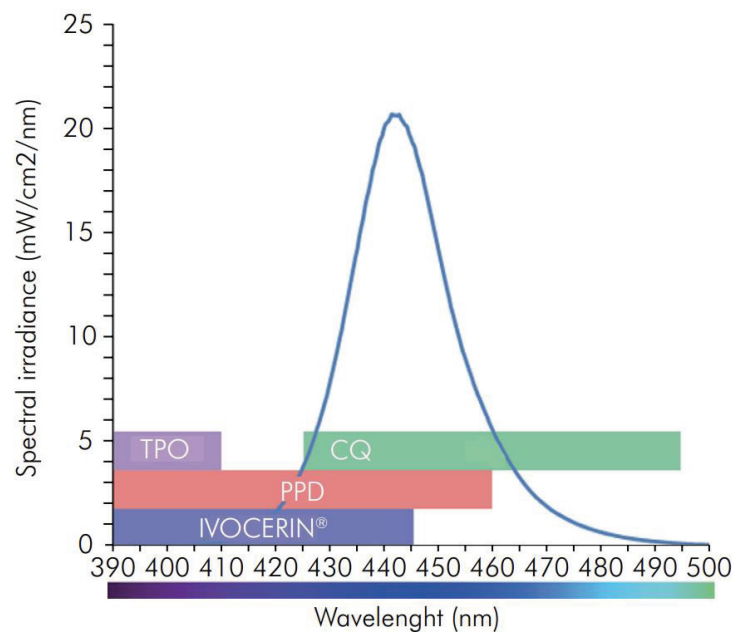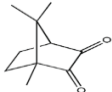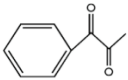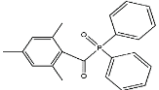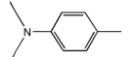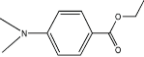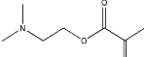
Figure 2.6 Absorption spectra of CQ, PPD, and TPO and emission spectrum of the blue LED (Source: Rueggeberg et al. 2017)

Ethyl 4- (dimethylamino)-benzoate (EDMAB) or dimethyl amino ethyl methacrylate (DMAEMA) are used as an accelerator together with CQ in the literature. EDMAB is more stable compared to DMAEMA, so it can be stored for longer periods of time without significant degradation or loss of activity. This makes it more convenient for manufacturers and ensures a consistent level of polymerization efficiency over time.

Molecular structures and main properties of commonly used initiators and accelerators are shown in Table 2.6 (Pratap et al. 2019).

Table 2.6 Main properties of commonly used initiators and co-initiators (Source: Pratap et al. 2019)

Type	Name	Molecular Structure	Color	Refractive Index	Absorbance (nm)	
					Range	Peak
Initiator	CQ		yellow	*	420-510	474
Initiator	PPD		white	1.53	300-480	410
Initiator	TPO		white	1.48	230-430	385
Accelerator	DMPT		white	1.54	NA	
Accelerator	EDMAB		transparent	1.53	NA	
Accelerator	DMAEMA		transparent	1.44	NA	

2.3.4 Coupling Agent
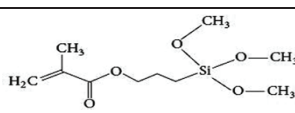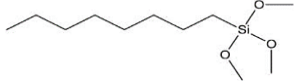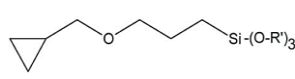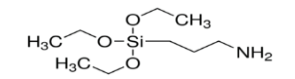
The bond between inorganic particles and organic polymer matrix is crucial to achieving the desired properties of resin-based dental composites. Especially mechanical performance of resin-based dental composites is largely dependent on the bonding. If the bond is strong, the stresses can be distributed and transferred from the matrix to the particles. Therefore, substances called silane coupling agents are often used to modify the filler particle surfaces. This surface modification provides a functional interface that allows covalent attachment between the resin matrix and the reinforcing filler particles with higher modulus. It also provides that the surface energy of the fillers is reduced.

Thus, the hydrophilicity and consistency of the composite paste are reduced while filler dispersion within the resin is enhanced (Cramer, Stansbury, and Bowman 2011).

Studies have reported that unmodified filler particles lead to a poor matrix-reinforcement interface, which can have a negative impact on the properties of the composite (H. Chen et al. 2018). It has been reported that this agent protects the filler against fracture and improves the stress transfer to harder inorganic filler particles. It is also known that it reduces the amount of water sorption and wear (Chaughule 2018).

There are many types of commercial silane coupling agents. The chemical structures of these agents are shown in Table 2.7. Those with unsaturated groups such as acrylate and methacrylate-based silane coupling agents can be copolymerized during curing thermoset resins. Thus, the inert filler turns into an active monomer and takes part formation of the final resin. (Lung and Matinlinna 2012). The most common silane coupling agent used is 3-methacryloxypropyltrimethoxysilane (γ-MPS) which is a methacrylate-based agent. The three methoxy groups in γ-MPS provide a large site for the agent to join with the filler. Moreover, its short chain length provides good mobility. Karabela and Sideridou compared the sorption properties of a dental nanocomposite consisting of a Bis-GMA/TEGDMA (50/50 wt%) matrix and silica nanoparticles silanized with various silanes. γ-MPS, OTMS, and a mixture of γ-MPS /OTMS (50/50 wt%) were used as the silanes. It has been observed that γ-MPS prevents the agglomeration of nanoparticles and allows the particle surface to be copolymerized with the matrix polymer by covalent bonding and hydrogen bonding. Thus, it supports interfacial adhesion (Karabela and Sideridou 2008).

Table 2.7 The chemical structures of silane coupling agents used in the literature

Silane	Chemical Nomenclature	Molecular Structure	Chemical Formulation
γ-MPS	3-methacryloxypropyl trimethoxysilane		$CH_2=CCH_3CO_2(CH_2)_3Si(OCH_3)_3$
OTMS	n-octyltrimethoxysilane		$CH_3(CH_2)_{17}Si(OCH_3)_3$
GPTMS	3-glycidoxypropyl trimethoxysilane		$CH_2(O)CHCH_2O(CH_2)_3Si(OCH_3)_3$
APTES	3-aminopropyl triethoxysilane		$H_2N(CH_2)_3Si(OC_2H_5)_3$

2.3.4.1 Surface Modification with Silane Coupling Agent

Silanes are indicated by X-Si-(OR)$_3$ chemical formulation. Here, X is the organofunctional group and R is the hydrolyzable alkyl group (methoxy). The first step of the surface modification is the hydrolysis of the alkyl group to the reactive silanol (Si-OH) groups by the following reaction:

X-Si-(OR)$_3$ + 3H$_2$O → X-Si-(OH)$_3$ + 3ROH
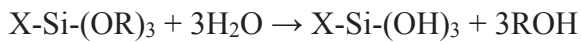
Then silanol groups can react with the surface hydroxyl (OH) groups of the fillers by the following condensation reaction (Matinlinna, Lung, and Tsoi 2018):

Substrate-OH + X-Si-(OH)$_3$ → Substrate-O-Si + H$_2$O
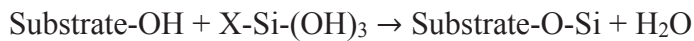
The strongest adhesion is achieved with materials such as silica and glass which can form strong siloxane (Si-O-Si) bonds via the condensation of surface hydroxyl groups on the substrate. On the other side, the organofunctional group (X) copolymerizes with the resin matrix. The chemical reaction of the silane coupling agent with fillers is given in Figure 2.7 (El-Banna, Sherief, and Fawzy 2019).
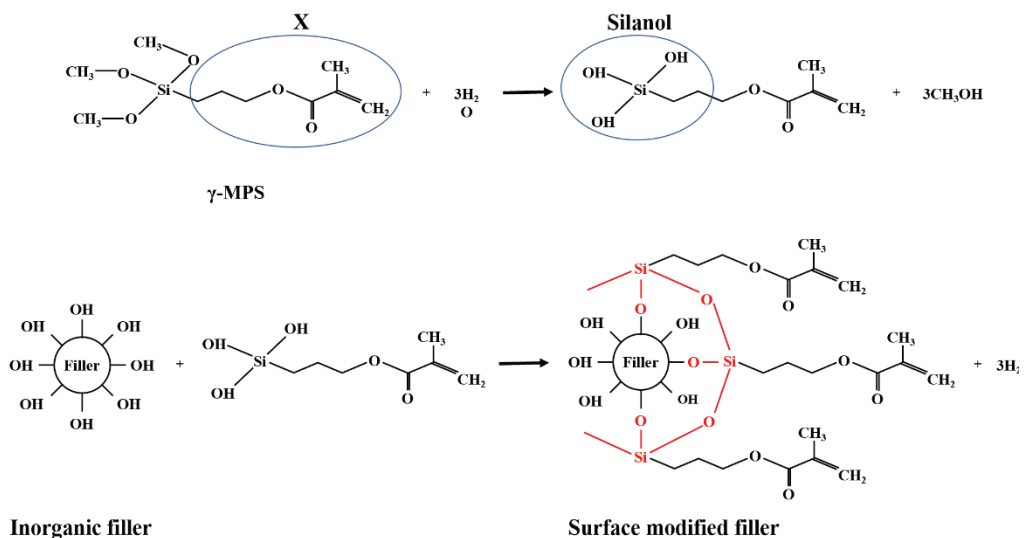
Figure 2.7 Chemical reaction of the silane coupling agent with filler (Source: Chaughule 2018)

Different methods are used for the surface modification of the filler particles with a silane coupling agent. Two main mechanisms are suggested in the literature. The first is the hydrolysis mechanism. In this mechanism, trialkoxysilanes X-Si-(OR)$_3$ are gradually hydrolyzed into silanol groups. Therefore, water is required for these processes. However, it is reported that the methoxy groups of γ-MPS hydrolyze very slowly in water. Because silanes dissolve easily in ethanol, a solution containing water and ethanol is often preferred. Higher pH causes the homopolymerization of the silanol groups into longer chains which hinders their mobility. Therefore, pH of the process is an important parameter and it should be adjusted to 2-6 by adding usually acetic acid. The rate of hydrolysis is fast in an acidic medium while it reaches a minimum in a neutral medium (Matinlinna, Lung, and Tsoi 2018). The silanol groups produced by hydrolysis of the silane condense with surface hydroxyl groups on inorganic particles and form a covalent siloxane bond.

Another mechanism is the direct condensation mechanism. In this mechanism, a catalyst such as an amine is used to accelerate the condensation reaction. The -OCH$_3$ of the silane condenses directly with the surface hydroxyl groups of the filler. Thus it bonds chemically to the inorganic filler particles (Sideridou and Karabela 2009). The advantage of using the direct condensation mechanism over the hydrolysis mechanism is the simplicity of the process. Direct condensation provides rapid and efficient surface modification. This can simplify the manufacturing process and reduce the time and cost required for surface modification (Plueddemann 1991).

The efficiency of the silanization process depends on the thickness of the silane film, which is controlled by the amount of silane used. A critical thickness of the silane layers should be achieved (El-Banna, Sherief, and Fawzy 2019). Excess silane can lead to the formation of a second layer of hydrogen bonded to the silane layer covalently bonded to the silica surface. This can impair the function of the silane molecules to bond the filler to the matrix (Sideridou and Karabela 2009). That's why, the amount of silane to be used for the modification process should be calculated by using the following equation:

$$X = \left(\frac{A}{W}\right) \times 100 \qquad (2.1)$$

Where X, A, and W represent the amount of γ-MPS to be used in percent by weight, the surface area of the inorganic filler particles in m^2/g, and surface coverage of silane per unit mass (for γ-MPS W=2525 m^2/g), respectively.

2.4 Polymerization Systems of the Resin-Based Composites

Composites are resin-based materials whose structures are largely composed of monomers and comonomer dimethacrylates. The monomers are in the form of carbon-carbon double bonds (C=C) before they become polymers. During their polymerization, these double bonds open and the monomers begin to form bonds with each other. In this way, polymer chains are formed. These composites are classified according to their polymerization mechanism.

2.4.1 Chemically-cured Composites

These structures are created using two pastes. First is a catalyst paste that includes benzoyl peroxide (BPO) as an initiator and the other one is a base paste that contains an aromatic tertiary amine, usually N,N-dimethyl-p-toluidine. The tertiary amine (TA) is necessary to decompose the breakdown of BPO at room temperature (El-Banna, Sherief, and Fawzy 2019).

2.4.2 Light-cured Composites

Light-cured composites were first introduced in the early-1970s. They initially required UV light sources operating at 360-400 nm to initiate polymerization. However, the use of UV light posed risks to the health of the eyes and oral tissues. Moreover, the depth of cure of UV-cured composites was limited. Quartz-Tungsten-Halogen (QTH) lights have been used. However, these light curing units have significant disadvantages

including a limited lifespan of 40-100 hours, high operating temperatures, and a significant amount of heat generated during curing. Alternative light sources such as argon laser, plasma light, and superbright blue light-emitting diodes (LEDs) have been proposed to eliminate the problems of halogen technology and visible light-cured composites were introduced in the late-1970s. This new photoinitiator system utilized camphorquinone (CQ) together with the tertiary amine (TA) co-initiator and provided a higher degree of conversion compared to chemically-cured composites (Santini 2010).

The photopolymerization reaction of CQ by light activation is given in Figure 2.8. CQ has an absorption range of 400 to 500 nm. The peak sensitivity is close to 470 nm in the blue part of the visible spectrum. CQ absorbs light and interacts with TAs to form a photoexcited complex resulting in free radicals on both CQ and TAs. This photoexcited complex is called as exciplex. Charge transfer from the nitrogen lone pair of the electron-donor amine to the activated carbonyl of CQ generates two radical ion species within the exciplex. If there is any available carbon in the amine, intermolecular H-abstraction produces two free radicals including a reactive aminoalkyl radical and a relatively unreactive camphorquinone ketyl radical (Cosola et al. 2019). These free radicals attack the carbon-carbon double bonds (C=C) of the monomers, creating new radicals with a longer polymer chain (propagation step). The propagation step continues until all of the monomers are consumed and the reaction process ends.

N,N-dimethyl-p-toluidine (DMPT) is one of the most commonly used co-initiator or accelerators, but it has been reported to be toxic. Therefore, ethyl 4- (dimethylamino)-benzoate (EDMAB) and/or dimethyl amino ethyl methacrylate (DMAEMA) are widely used in the literature together with CQ (Cosola et al. 2019).

2.4.3 Dual-cured Composites

Two pastes are used similar to chemically-cured composites. One of these pastes is the base and the other is the catalyst. Similar to light-cured composites, base paste contains a CQ/TA photoinitiator system. An aromatic TA is also available. When these pastes are mixed, chemically curing occurs very slowly. It is accelerated by light curing. The main advantage of this system is that complete curing is guaranteed even if light curing is insufficient. The biggest disadvantage is that when the two pastes are mixed,
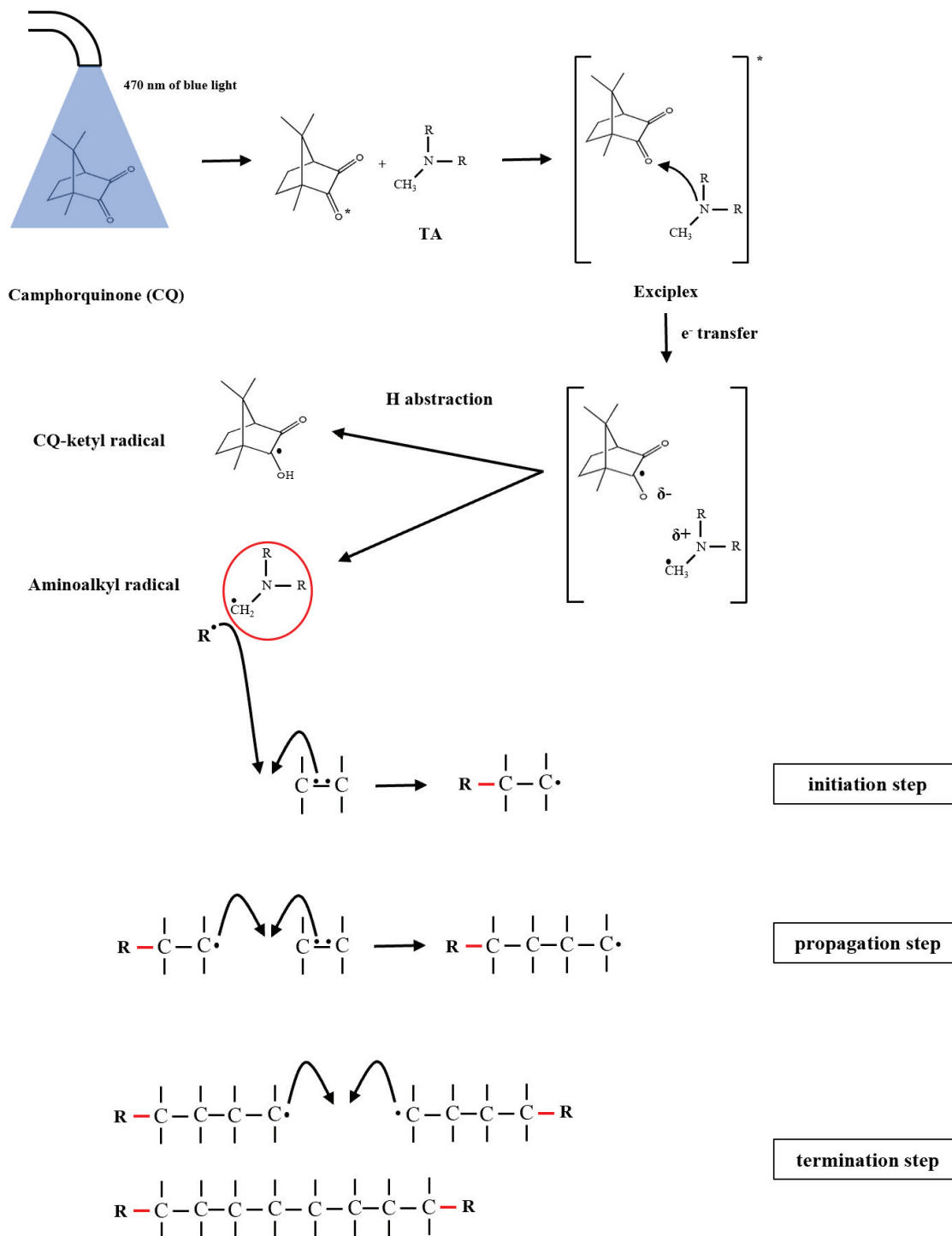
Figure 2.8 Photopolymerization of CQ (Source: Cosola et al. 2019)

pores occur. It is thought that this problem can be largely solved if mixing syringes are used (Santini, Gallegos, and Felix 2013).

2.5 Properties of Resin-Based Dental Composites

Restorative materials are adversely affected by parameters such as temperature and pH changes and different forces in the mouth, which is a dynamic environment. The restorative material to be selected should be capable of regaining the lost chewing function and aesthetics. The success and longevity of restorations depend on factors such as the properties of the light source used, the application technique of the dentist, the cavity design in the teeth, and especially the properties of the restorative material.

2.5.1 Degree of Conversion

The degree of conversion (DC) is known as the degree to which monomers participate in the reaction to form polymers or the percentage of carbon-carbon double bonds (C=C) that have been converted to carbon-carbon single bonds (C-C) during the polymerization. The high percentage is an essential material property to achieve optimum physical and mechanical properties and has a crucial effect on a successful composite restoration. It strongly affects properties such as strength, modulus of elasticity, hardness, water sorption and solubility, color stability, resultant microleakage, and secondary caries.

The degree of conversion is influenced by various factors, including the size and amount of filler particles, the type and amount of monomers, the type and concentration of the initiator, the shade and translucency of the material, the intensity and wavelength of the light source, the distance between the light source and composite surface and the duration of the irradiation. During polymerization, it is desired to convert all resin monomers into polymer. However, the conversion degree is never 100%. It is about 50%-75% for conventional composites (J. L. Ferracane et al. 2017).

Bis-GMA, the most widely used monomer in modern commercial composites, has advantages such as relatively low polymerization shrinkage, fast curing, and strong and rigid polymeric networks. However, its high viscosity restricts mobility during polymerization, which hinders the polymer from reaching high degrees of conversion (DC). Comonomers based on Bis-EMA, which have a higher molecular weight and lower viscosity, typically exhibit higher DC compared to Bis-GMA/TEGDMA resin mixtures (Miletic 2018).

DC decreases gradually with increasing increment thickness of the composite resin because the light is weakened by absorption and scattering. The curing light intensity that reaches the bottom of a composite layer is significantly lower than the intensity that reaches its surface. Currently, the depth of cure of light curing units does not exceed 2 mm. Radiation exposure decreases as the distance between the surface of the composite and the curing tip increases. This reduction in exposure may be due to the height of the curing tip and the depth of the cavity being treated. A 50% reduction in light irradiation has been reported when the curing distance is increased from 0 to 6 mm (El-Banna, Sherief, and Fawzy 2019).

2.5.2 Polymerization Shrinkage

Polymerization shrinkage is one of the main problems with resin-based composite restorations that have been the subject of considerable research since composites were first introduced. This shrinkage occurs because monomer molecules convert into a polymer network and it results in the replacement of van der Waals interactions with covalent bonds. The monomer molecules in the matrix are then packed more tightly into a three-dimensional cross-linked network structure, reducing the distance between them from 4 to about 1.5 Å. As a result, dimethacrylate-based composites experience volumetric shrinkage of approximately 2-6% during polymerization, which can result in poor adaptation to the cavity walls, postoperative pain, and recurrent caries. Despite efforts, modern bonding systems have not been able to provide a reliable bond between the resin-based composite and the tooth. Studies have shown that about 90% of shrinkage occurs in the first hours, especially in the first 30 minutes (Kleverlaan and Feilzer 2005).

The bonding of resin-based dental composites to the tooth structure limits the strain that the material can withstand, so shrinkage leads to stresses. These stresses result in restoration fractures. In addition, marginal leakage may occur due to shrinkage and secondary caries may occur. In this case, clinical failure of the restoration takes place again. A schematic representation of these problems is given in Figure 2.9.
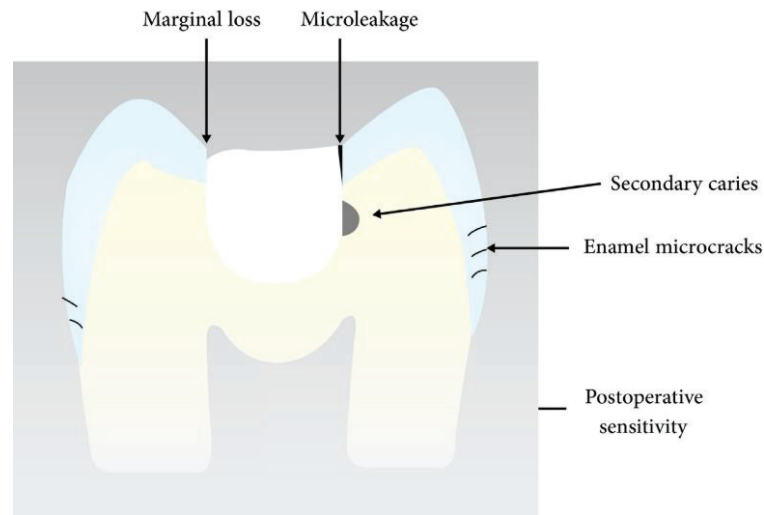
Figure 2.9 The problems related to polymerization shrinkage

The amount of inorganic filler and molecular weight of the monomer system are the factors affecting shrinkage in resin-based dental composites. Increasing the amount of filler can reduce the amount of shrinkage by decreasing the amount of resin matrix. Monomer chemistry also plays an important role in shrinkage. Diluent monomers, such as TEGDMA, have lower molecular weight compared to Bis-GMA. Therefore, increasing the amount of polymerizable carbon-carbon double bonds with the use of diluents leads to greater shrinkage.

The incremental layering technique is highly recommended for the placement of resin composites because it reduces the effects of shrinkage stresses, increases bond strength, and reduces interfacial microleakage and postoperative pain. However, it is important to ensure sufficient light penetration and maximum depth of cure during placement using this technique. There is a risk of voids between layers and extended curing times (El-Banna, Sherief, and Fawzy 2019).

2.5.3 Mechanical Durability

The longevity of dental restorations depends on various factors including the material used, patient-related factors such as oral hygiene, chewing abilities, and abnormal habits, dentist-related factors such as skills and techniques, as well as cavity size and complexity. Despite the challenges in improving the clinical performance and durability of resin-based dental composites, recent advancements in these materials significantly enhanced their clinical performance (El-Banna, Sherief, and Fawzy 2019).

In general, current resin-based dental composites exhibit satisfactory mechanical behavior for use in most clinical restorative procedures. However, it still needs to be developed. The main causes of failure within the first 4 years of service are fracture and secondary caries. That's why, many different techniques have been applied to increase fracture toughness and especially flexural strength in the literature. In composites, the size and composition of the fillers have been associated with these properties. They depend on the filler load including the amount, type, size, distribution of fillers, and the bond between these fillers and the matrix. In vitro studies have shown that the higher the filler load, the higher the strength, hardness, and toughness (El-Banna, Sherief, and Fawzy 2019). Additionally, hybrid and nano-filled composites have been found to have significantly higher fracture toughness (K_{IC}) than that of micro-filled composites (Zhou et al. 2019).

2.5.4 Water Sorption and Solubility

The resin matrix composition, the type and amount of filler particles used, the degree of conversion, and the interface between filler and matrix are the main factors affecting the water sorption and solubility properties of dental composites. It has been reported that water sorption and solubility of the composite increase when hydrophilic monomers such as hydroxyethyl methacrylate (HEMA) are used, but it decreases when bisphenol A-glycidyl methacrylate (Bis-GMA) and urethane dimethacrylate (UDMA) are used. If a large amount of filler is added, the amount of resin matrix available for water

uptake will decrease, and water sorption and solubility properties will be positively affected (Domingo et al. 2001).

Insufficient light-curing intensity and duration can result in inadequate polymerization, particularly in deeper layers of resin composites. Inappropriately composites tend to have higher water sorption and solubility, which can cause premature discoloration in clinical settings (El-Banna, Sherief, and Fawzy 2019).

The distribution of particles in the resin matrix should be homogeneous. Aggregation of particles can provide easy diffusion pathways, potentially creating voids or weak zones that increase water sorption and solubility. As the particle size decreases, the surface area to volume ratio increases. This can lead to greater interactions with water and potentially increase water sorption. The bond between the filler particles and the resin matrix is also an important factor affecting water sorption and solubility. If there is poor adhesion between the filler and the matrix, water may enter the interface and cause deterioration. Appropriate surface treatment of filler particles, such as silane coupling agents, can improve bonding and reduce water sorption and solubility (Santos et al. 2002; Liu, Jiang, et al. 2014).

2.5.5 Adaptation

For restoration treatment with direct resin-based dental composite, the microleakages caused by marginal cavities must be prevented because it leads to the formation of secondary caries. With the use of low viscosity materials, wettability can be increased and adaptation improved, thus microleakage can be reduced. However, these materials have relatively lower flexural strength or modulus of elasticity. In order to improve the adaptation of the composite, one approach is to decrease its viscosity during application while maintaining its mechanical properties. Preheating the composite can significantly decrease its viscosity. At high temperatures, the thermal vibrations cause the monomers to separate, allowing them to slide past each other more easily and reducing internal friction (El-Banna, Sherief, and Fawzy 2019).

It has been reported that there is a relationship between the margins of the restoration and the stickiness of the material. It is important that the composite adheres to the cavity walls while not sticking to the plugger. The adhesion between the plugger and

the composite is created at the molecular level through weak dipole (van der Walls) interactions. This may cause the material to pull back from the cavity during restoration application and the shape and marginal integrity of the restorations may be negatively affected. Low stickiness is also important to facilitate the transfer of the material from the packaging to the prepared cavity (Loumprinis et al. 2020).

Some studies involve lowering and lifting a stainless steel probe flat tip onto the resin composite to see the stickiness. The degree of stickiness is determined by the height of the material when the steel plugger is pulled until it separates from the composite (Ertl et al. 2010).

2.5.6 Aesthetic Properties

The restoration of anterior teeth for aesthetic purposes can be challenging due to the complex optical properties of enamel and dentin. Enamel is highly translucent with approximately 70% light transmittance, while dentin is opaque with 52% light transmittance. Several factors, including material properties such as shade, fluorescence, translucency, wear resistance, and gloss retention, as well as technical factors such as tooth preparation design, proper adaptation protocol, and anatomical shaping and contouring, contribute to the success of the aesthetic restoration. The translucency and color of composites are determined by various factors such as the composition, pigments, filler size and amount, compatibility of refractive index between fillers and matrix, resin type, and curing quality (El-Banna, Sherief, and Fawzy 2019).

2.5.7 Radio-opacity

Resin composites must have high opacity to X-rays (high energy photons), also known as radio-opacity, to be an effective restorative material for diagnosing secondary caries. Because, the restorative material must be clearly distinguished from impaired tissue and X-ray imaging is the main diagnostic tool (Heintze and Zimmerli 2011).

X-ray absorption is connected with the atomic number of the atoms encountered. According to ISO 4049, the absorption of a 1 mm thick pure aluminum layer (atomic no, $Z = 13$) indicates minimum radio-opacity for composites. Because the contribution of the resin phase of the composites to X-ray absorption is low, these composites should contain highly radio-opaque fillers composed of heavy elements such as barium ($Z = 56$), strontium ($Z = 38$) and zirconium ($Z = 40$). On the other hand, caries appear more radio-transparent because they are demineralized. Barium is the most widely used filler for this purpose. Current commercial dental restorative composites provide ISO requirements in terms of radio-opacity (Miletic 2018). Radio-opacity of different restorative materials including nanohybrid composite and amalgam is given in Figure 2.10.

Figure 2.10 Radio-opacity of different restorative materials 1) nanohybrid composite and 2) amalgam (Source: Heintze and Zimmerli 2011)

CHAPTER 3

EXPERIMENTAL

3.1 Experimental Design

The aim of this study is to examine the single effects and cross-effects of zirconia and hydroxyapatite (HA) particles on the mechanical properties, water sorption and solubility properties of dental composites. The amount of zirconia and HA nanoparticles were considered as variables. For this reason, full factorial experimental design, which gives the opportunity to examine the interaction of factors with each other, was used. The factors and levels for a 3^2 full factorial experimental design were shown in Table 3.1.

Table 3.1 Factors and levels for full factorial experimental design

Factors	Levels			Response
ZrO$_2$	0 wt.%	1 wt.%	2 wt.%	Flexural Strength
HA	0 wt.%	3 wt.%	5 wt.%	Compressive Strength

The experimental design used in this study is given in Table 3.2. The required composite number was calculated as 9. After the composites were prepared, they were molded in accordance with ISO 4049 standard. Three-point bending and compression tests were performed using Shimadzu Autograph AGJ-S universal test machine. In addition, water sorption, and solubility, and depth of cure values were evaluated according to ISO 4049 standard.

Table 3.2 Full factorial experimental design

| Experiment No | Factors | | Sample Code |
	HA (wt.%)	ZrO$_2$ (wt.%)	
1	0	0	REF
2	3	0	H3
3	5	0	H5
4	0	1	Z1
5	0	2	Z2
6	3	1	H3Z1
7	3	2	H3Z2
8	5	1	H5Z1
9	5	2	H5Z2

3.2 Materials

In this study, high molecular weight monomers which are called Bis-EMA (ethoxylated bisphenol A glycol dimethacrylate) and UDMA (urethane dimethacrylate), and a diluent TEGDMA (triethylene glycol dimethacrylate) were used for resin mixture. Because its absorption range is closest to the emission spectrum of the LEDs, CQ (camphorquinone) was used as the initiator. EDMAB (ethyl 4- (dimethylamino)-benzoate), which is the most common accelerator used together with CQ in the literature, was preferred. The chemicals used for the resin mixture and their supplier information are given in Table 3.3.

Table 3.3 Chemicals used for resin mixture and their supplier information

Properties / Chemicals	Molecular Weight (g/mol)	CAS No	Supplier
Bis-EMA	376.4	41637-38-1	Sigma-Aldrich, Germany
UDMA	470.56	72869-86-4	Sigma-Aldrich, Germany
TEGDMA	286.32	109-16-0	Sigma-Aldrich, Germany
CQ	166.22	10373-78-1	Sigma-Aldrich, Germany
EDMAB	193.24	10287-53-3	Sigma-Aldrich, Germany

As inorganic filler particles, hydrophilic fumed silica CAB-O-SIL® M-5, colloidal silica MP 1040, zirconia, HA, and barium glass particles were chosen for resin-based dental composites. These inorganic filler particles used in dental composites and their supplier information are given in Table 3.4.

Table 3.4 Filler particles used in dental composites and their supplier information

Properties / Chemicals	Average Particle Size (nm)	BET Surface Area (m^2/g)	CAS No	Supplier
Fumed silica (CAB-O-SIL® M-5)	200	200	112945-52-5	Cabot Corporation, USA
Colloidal silica (MP-1040)	100	31	7631-86-9	Nissan Chemical Industries, Ltd., Japan
Zirconia	20-30	35	1314-23-4	Skyspring Nanomaterials. Inc., USA
Hydroxyapatite	200	9.4	12167-74-7	Sigma-Aldrich, Germany
Barium Glass	700	-	65997-17-3	Schott Ag Landshut, Germany

For surface modification of the inorganic filler particles except for barium glass; γ-MPS (3-methacryloxypropyltrimethoxysilane) as silane coupling agent, cyclohexane as solution, and n-propylamine as catalyst were used. These chemicals used for surface modification and their supplier information are given in Table 3.5. Because barium glass particles are already treated with γ-MPS, they were used as-received.

Table 3.5 Chemicals used for surface modification and their supplier information

Properties / Chemicals	Molecular Weight (g/mol)	Density (g/cm^3)	CAS No	Supplier
γ-MPS	248.35	1.045	2530-85-0	Sigma-Aldrich, Germany
Cyclohexane	84.16	0.779	110-82-7	Sigma-Aldrich, Germany
n-propylamine	59.11	0.719	107-10-8	Sigma-Aldrich, Germany

3.3 Surface Modification of Inorganic Fillers

Firstly, the surface modification or silanization process was carried out so that the bond between the inorganic particles and the organic resin matrix is strong and thus the composite can provide the desired properties. γ-MPS is recommended for surface modification of silica, zirconia, and HA particles in the literature (Karabela and Sideridou 2008; Wang et al. 2020; Labella, Braden, and Debt 1994). The amount of γ-MPS to be used is a very important factor for surface modification to be carried out efficiently. For this reason, the amount of silane to be used for each particle was calculated by using Equation (2.1) and given in Table 3.6.

Table 3.6 Calculated amount of silane for efficient surface modification

Inorganic Filler Type	Specific Surface Area (m^2/g)	Amount of γ-MPS (wt.%)
Fumed silica	200	7.92
Colloidal silica	31	1.23
Zirconia	35	1.39
Hydroxyapatite	9.4	0.37

For the surface modification of the inorganic filler particles, a direct condensation mechanism was used. In this mechanism, 100 ml of cyclohexane solution for each particle type was mixed with 0.1 g of n-propylamine which was added as a catalyst to accelerate the reaction. Then, the calculated amount of silane given in Table 3.6 was added. Finally, 5 g of particles for each particle type were added separately into this mixture. They were then mixed with MTOPS MS300 HS magnetic stirrer with a speed of 400 rpm for 30 min at room temperature and then at 60 ºC for another 30 min. Then, this mixture was dried at 80 ºC for 24 hours to remove the solution and volatile by-products.

3.4 Preparation of Dental Composites

The total particle amount was kept constant at 65% by weight for all samples. Inorganic filler contents of the prepared resin-based dental composites are given in Table 3.7. First, resin mixtures containing 40/30/30 Bis-EMA, TEGDMA, and UDMA in terms of weight ratio, respectively, were prepared for all the composites. For the preparation of the composite pastes, beakers covered with aluminum foil were used to prevent unwanted polymerization reaction caused by ambient light. CQ (0.2 wt.%) as initiator and 4-EDMAB (0.8 wt.%) as the accelerator was added into the resin mixture. These resin mixtures were stirred in an ultrasonic bath at 50 ºC for 15 minutes to obtain a homogeneous dispersion.

Table 3.7 Inorganic filler contents of the prepared resin-based dental composites

Sample No	Inorganic Filler Particles (wt.%)					
	Ba Glass	Fumed SiO_2	Colloidal SiO_2	HA	ZrO_2	Total
REF	25	15	25	0	0	**65**
H3	25	15	22	3	0	**65**
H5	25	15	20	5	0	**65**
Z1	25	15	24	0	1	**65**
Z2	25	15	23	0	2	**65**
H3Z1	25	15	21	3	1	**65**
H3Z2	25	15	20	3	2	**65**
H5Z1	25	15	19	5	1	**65**
H5Z2	25	15	18	5	2	**65**

After ensuring the homogeneity of the resin mixture, 25 wt.% of modified barium glass particles were added in accordance with the literature. Then fillers other than fumed silica were added at the rates which are given in Table 3.7 into composites and they were stirred manually by hand spatulation. Fumed silica has a high surface area. This makes it difficult to disperse in the resin by hand spatulation method or using an ultrasonic bath. Therefore, fumed silica was stirred by hand spatulation only in an amount that will facilitate the handling of the composite and the composite pastes were transferred to the

mortar mill where dispersion was accomplished using a mortar mill. As suggested by Khaje & Jamshidi, the amount of fumed silica was kept constant at 15 wt% for all composites. The composites were stirred for a total of 20 minutes with the help of a RETSCH RM 200 mortar mill until homogeneity was achieved. Before each use, the mortar was heated in an oven at 80 °C for 15 minutes. The consistency of the composite pastes at each stage is shown in Figure 3.1.

Composite pastes were placed into the molds for the tests to be carried out. The mold was first placed on the transparent film. A frekote mold release agent was used to easily remove the sample from the mold. Then the composite paste was placed into the mold. The mold was slightly overfilled to remove air bubbles. Then another transparent film was put on it and pressure was applied by using a flat object so that the excess material can come out of the mold. Then all test specimens were cured on both sides for 30 seconds by using LITE-Q Auto Ramp-Up LD-107 light curing unit with a wavelength of 450-470 nm and luminosity of up to 1000 mW/cm^2. Prepared samples were stored in a desiccator for 24 hours before testing. A schematic representation of the composite preparation procedure is given in Figure 3.2.

| Bis-EMA/UDMA/TEGDMA + CQ + EDMAB mixture after ultrasonic bath | After addition of fillers other than fumed SiO$_2$ by hand spatulation |
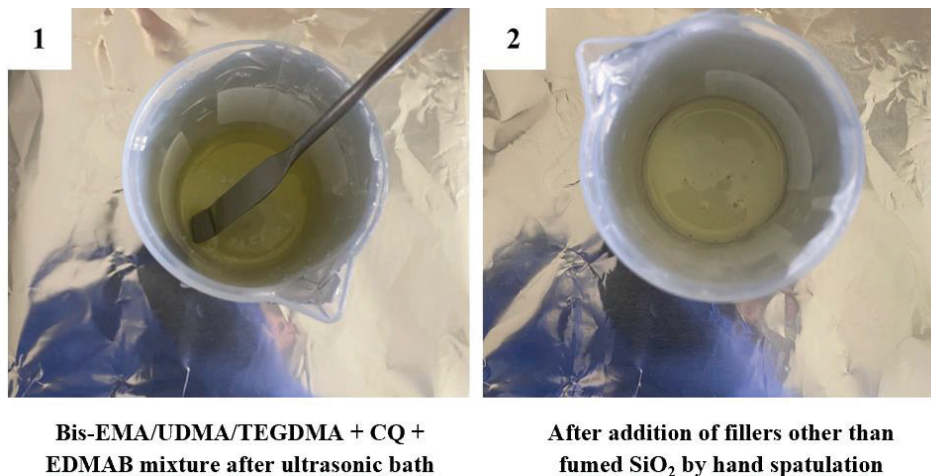
Figure 3.1 The consistency of the composite pastes at each stage
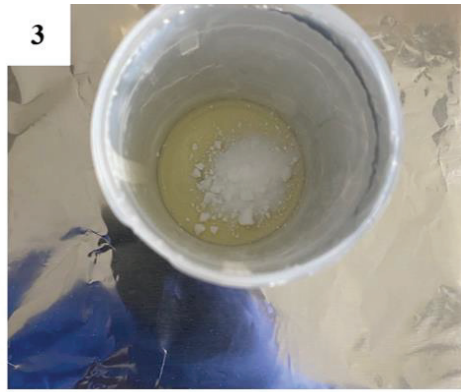
Addition of fumed SiO₂ by hand spatulation in an amount that will facilitate the handling
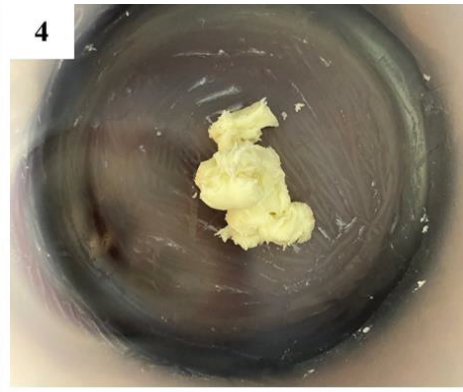
Transfer of the composite to mortar mill after addition of fumed SiO₂ by hand spatulation
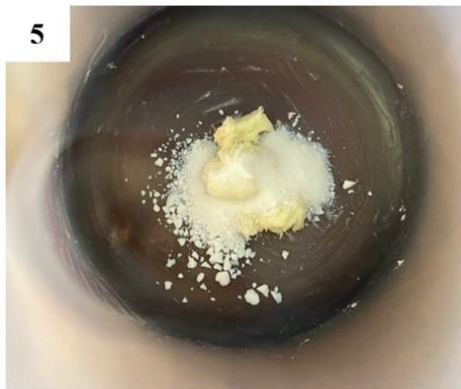
Consistency of the final composite
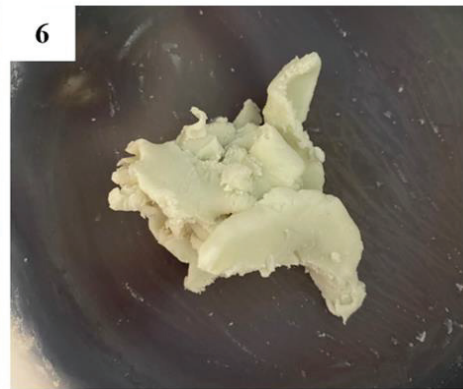
Addition of all fumed SiO₂ in mortar mill

Figure 3.1 (cont.)
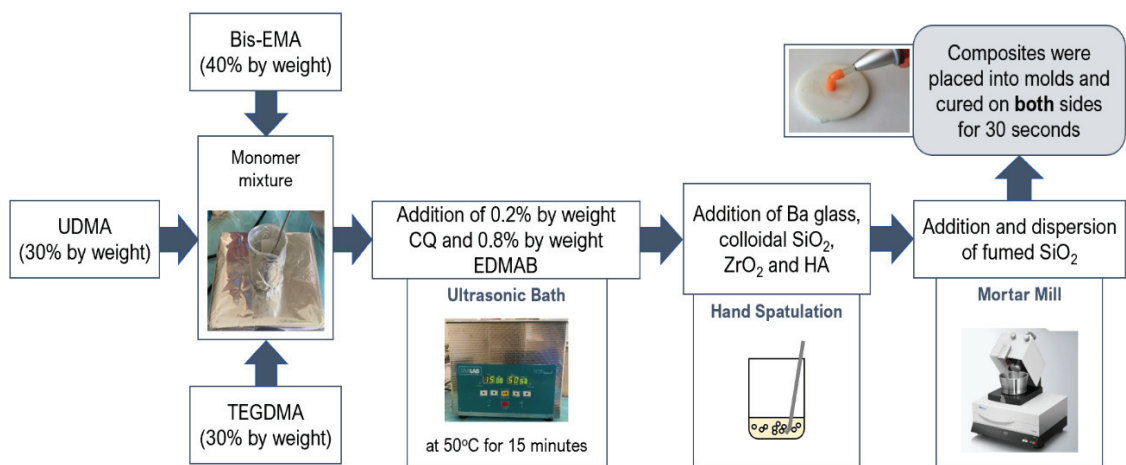
Figure 3.2 Schematic representation of the composite preparation procedure

3.5 Characterization of Dental Composites

Particles and composites were characterized by using Scanning Electron Microscopy (SEM), Dynamic Light Scattering (DLS) and Fourier Transform Infrared Spectroscopy (FTIR).

3.5.1 Scanning Electron Microscopy (SEM)

The surface morphology of the inorganic filler particles used in this study was analyzed with Scanning Electron Microscopy (SEM), FEI QUANTA 250 FEG. For SEM analysis, all the particles were dried in an oven at 100 °C for 1 hour to evaporate water. Conductive carbon tapes were used to mount the specimen onto a stub, allowing charges to dissipate through the tape, thus eliminating the charging problem.

In addition, fracture surfaces of the flexural strength specimens were observed by SEM to see particle distribution and whether there are porosity formations that will encourage damage in the composite and to gain insight into the cause and location of failure. The surfaces of all specimens were gold-coated by a sputtering apparatus before SEM examination.

3.5.2 Dynamic Light Scattering (DLS)

The average particle size and particle size distribution of the particles used except for zirconia were measured with Particulate Systems NanoPlus Particle Size Analyzer as a function of volume %. Malvern Zetasizer Nano ZS was used for zirconia nanoparticles. Dynamic Light Scattering (DLS) technique was used for the analysis with a laser light which has 660 nm wavelength. Particle size distribution was analyzed by preparing a suspension. For the analysis to be performed correctly, the suspension concentration should be 0.01-5 wt% and the particles should only be dispersed without dissolving in the solvent. Therefore, 0.01 g of zirconia nanoparticles were dispersed in 10 ml water by

adding Tween 80 as a surfactant, and 1 g of other particles were dispersed in 10 ml ethanol separately. They were kept in an ultrasonic bath for 30 minutes.

3.5.3 Fourier Transform Infrared Spectroscopy (FT-IR)

Fourier transform infrared (FTIR) analysis was performed to control whether the surface modification of the γ-MPS treated particles had taken place successfully. In order to see whether the surface modification was carried out properly or not, functional groups in unmodified and modified particles for all the inorganic filler types were analyzed by using FTIR instrument. ATR FTIR spectra were recorded in the wavelength range of $4000–400$ cm^{-1} and a resolution of 4 cm^{-1} at 20 scans per spectrum by using PERKIN ELMER Spectrum Two in the transmittance mode. Before FT-IR spectra analysis, all samples were dried and stored in a desiccator.

3.6 Mechanical Tests of Dental Composites

Given that fracture is the most common cause of failure of dental restorations, improved mechanical properties of resin-based composites are essential for long-term clinical applications of these materials. Flexural strength (σ_f), flexural modulus (E_f), and compressive strength (CS) were measured to evaluate the reinforcing effect of zirconia and HA when used individually and together.

3.6.1 Three-Point Bending Test

In a three-point bending test, a test specimen is subjected to a load at its center, resulting in compression on the upper surface and tension on the bottom surface of the specimen. During the test, force, and displacement values are measured. A schematic representation of the three-point bending test setup was shown in Figure 3.3.

Five specimens with the dimensions of (25±2) mm × (2.0±0.1) mm× (2.0±0.1) mm for each material were prepared according to ISO 4049 standard. For the preparation, a two-piece stainless steel mold was used.
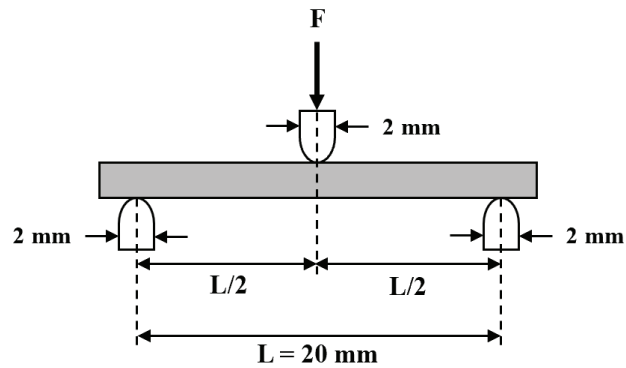
Figure 3.3 Schematic representation of the three-point bending test setup

The schematic representations of the mold and top view of irradiation zones for the preparation of the flexural strength test specimens are shown in Figure 3.4. The two-piece stainless steel mold and flexural strength test specimens taken from the mold are shown in Figure 3.5.
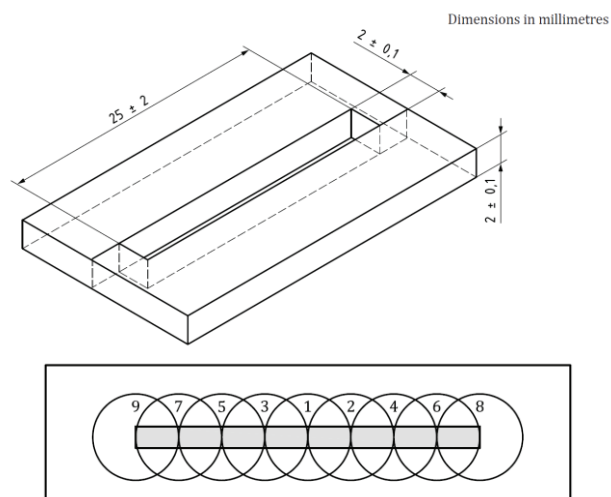
Figure 3.4 Dimensions of the mold and top view of irradiation zones for the preparation of the flexural strength test specimens
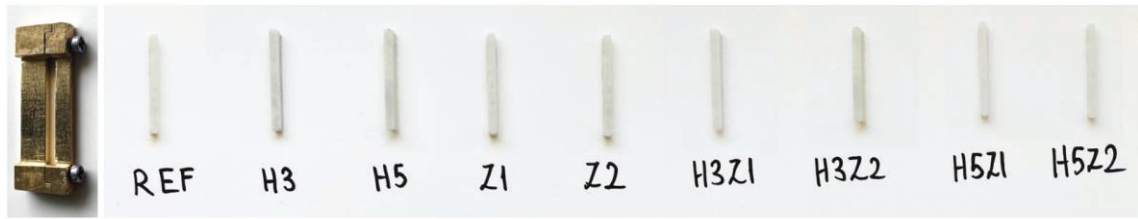
Figure 3.5 Two-piece stainless steel mold and flexural strength test specimens taken from the mold

Three-point bending test was performed using Shimadzu Autograph AGJ-S universal test machine. The span length was adjusted as 20 mm and rods with a diameter of 2 mm were used as the supports according to the standard. The dimensions of the samples were measured with an accuracy of 0.01 mm from the center. A load was applied to the sample at a crosshead velocity of 0.75 mm/min. The maximum load applied to the specimen at the fracture point was recorded. The flexural strength specimen during the test is shown in Figure 3.6.
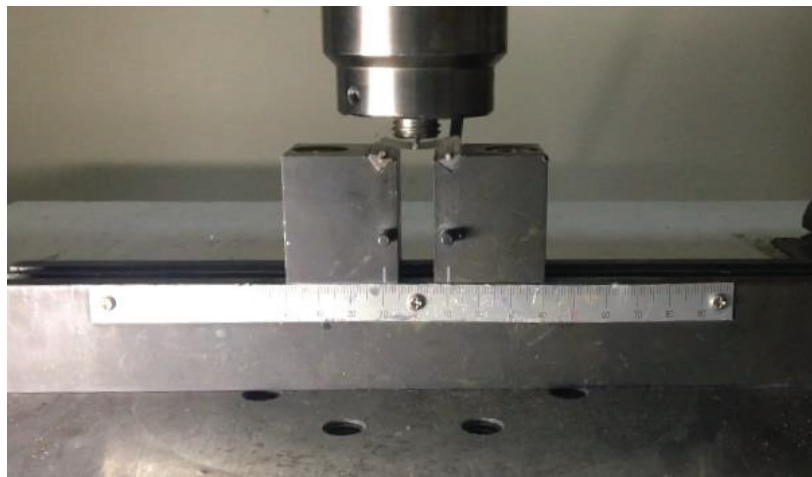
Figure 3.6 Flexural strength specimen during the test

The flexural strength (σ_f) and flexural modulus (E_f) of the dental composites were calculated from the following equations:

$$\sigma_f = \frac{3FL}{2bh^2} \tag{3.1}$$

$$E_f = \frac{F_1L^3}{4bh^3d} \tag{3.2}$$

Where F is the maximum load applied in Newton, L is the distance between the supports in mm, b is the width of the specimen in mm, h is the height of the specimen in mm and d is the displacement of the specimen during the test at load F_1 in mm.

3.6.2 Compression Test

In order to obtain the compressive strength (CS) of the dental composites, five specimens with a diameter of 4 mm and a height of 6 mm were prepared. The two-piece stainless steel mold used and prepared compression test specimens are shown in Figure 3.7. Compression test was performed using Shimadzu Autograph AGJ-S universal test machine at a crosshead velocity of 0.75 mm/min. The diameters of the samples were measured with an accuracy of 0.01 mm. The maximum load applied to the specimen at the fracture point was recorded. The compressive strength was calculated by dividing the maximum load at the fracture point F, by the cross-sectional area A of the specimen. *R* is the diameter of the specimen in mm.

$$CS = \frac{F}{A} = \frac{F}{\frac{\pi R^2}{4}} \tag{3.3}$$

Figure 3.7 Two-piece stainless steel mold and prepared compression test specimens

45

3.7   Depth of Cure Examination of Dental Composites

Three specimens with a diameter of 4 mm and a height of 6 mm were prepared in the same way as the compressive strength specimens according to ISO 4049. After the irradiation was completed, the sample was removed from the mold and uncured material was removed with the help of a spatula. The height of the cured cylinder material was measured with a caliper with an accuracy of 0.1 mm. The value obtained was divided by two according to the standard. All three values should not be less than 1.0 mm for opaque-toned restorative materials and 1.5 mm for all other materials.

3.8   Water Sorption and Solubility Test of Dental Composites

Water sorption and solubility test were performed according to ISO 4049 standard. Five specimens with a diameter of 15 mm and a thickness of 1 mm were prepared by overlapping irradiation for 30 seconds. Top view of overlapping irradiation zones is given in Figure 3.8.
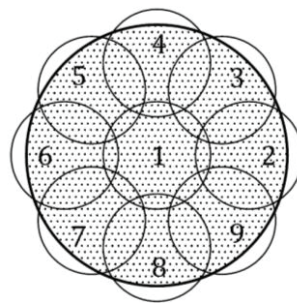
Figure 3.8 Top view of overlapping irradiation zones for the preparation of the water sorption specimens

Water Sorption and solubility specimens are shown in Figure 3.9. The specimens were dried in an oven at 37 °C for 24 hours and then kept in a desiccator at room temperature for 2 hours. Then, it was weighed with an accuracy of 0.1 mg and this process

was repeated until a constant mass is obtained. This resulting constant mass was recorded as m_1. This process took 1 week. In addition, the mean diameter and thickness were measured at this stage to calculate the volume of the specimen. Two measurements were made at right angles of the specimens to each other with an accuracy of 0.01 mm and the mean diameter was calculated. The thickness was measured with an accuracy of 0.01 mm at the center of the specimen and four equally spaced points on the periphery.

Figure 3.9 Water sorption and solubility test specimens

The specimens then were immersed in separate beakers containing 10 ml of distilled water at 37 °C and placed in an oven at 37 °C for 1 week. After 1 week, the specimens were removed and washed with distilled water. Surface water was wiped off until it was free from visible moisture. The specimens were waved in the air for 15 seconds and weighed. The resulting mass was recorded in m_2. Finally, the specimens were dried again in an oven at 37 °C for 24 hours and then left in a desiccator for 2 hours. Then, it was weighed with an accuracy of 0.1 mg and this process was repeated until a constant mass is obtained. The resulting constant mass was recorded in m_3. Water sorption (W_{sp}) and solubility (W_{sl}) were calculated by using Equation (3.4) and (3.5), respectively.

$$W_{sp} = \frac{m_2 - m_3}{V} \tag{3.4}$$

$$W_{sl} = \frac{m_1 - m_3}{V} \tag{3.5}$$

Where m_1 is the mass of the specimen before the immersion in water, m_2 is the mass of the specimen after the immersion in water, m_3 is the new mass of the specimen and V is the volume of the specimen. According to ISO 4049 standard, water sorption should be equal to or less than 40 µg/mm^3 and solubility should be equal to or less than 7.5 µg/mm^3.

CHAPTER 4

RESULTS AND DISCUSSION

4.1 Characterization Results of Dental Composites

In this chapter, the microstructural and physical properties of the dental composites prepared are presented. Characterization of the fillers used in the composites is also reported.

4.1.1 Scanning Electron Microscopy (SEM)

SEM images of untreated hydrophilic fumed silica and colloidal silica nanoparticles at magnifications of 100,000x and 400,000x are shown in Figure 4.1. Fumed silica nanoparticles were found to have irregular shape while colloidal silica particles have an evident spherical shape. Because fumed silica particles have a high specific surface area, they are prone to agglomeration due to van der Waals forces and hydrogen bonding between silanol (Si-OH) groups present on the particle surfaces. This agglomeration can create an interconnected porous network that makes the particles appear smaller and more irregular than their actual primary size as shown in Figure 4.1 (a) and (b). The average particle size of colloidal silica with a spherical shape was measured to be around 100 nm as seen in Figure 4.1 (d).

SEM images of untreated zirconia and HA nanoparticles at magnifications of 100,000x and 200,000x are shown in Figure 4.2. Zirconia nanoparticles were found to have a spherical shape with an average particle size of 30 nm as shown in Figure 4.2. They are aggregated into clusters. The morphology of HA particles is also spherical and they are aggregated into clusters like zirconia nanoparticles. Although there are small particles with an average particle size of 50 nm, it has also been observed that there are large particles close to 0.7 µm as shown in Figure 4.2 (c) and (d).
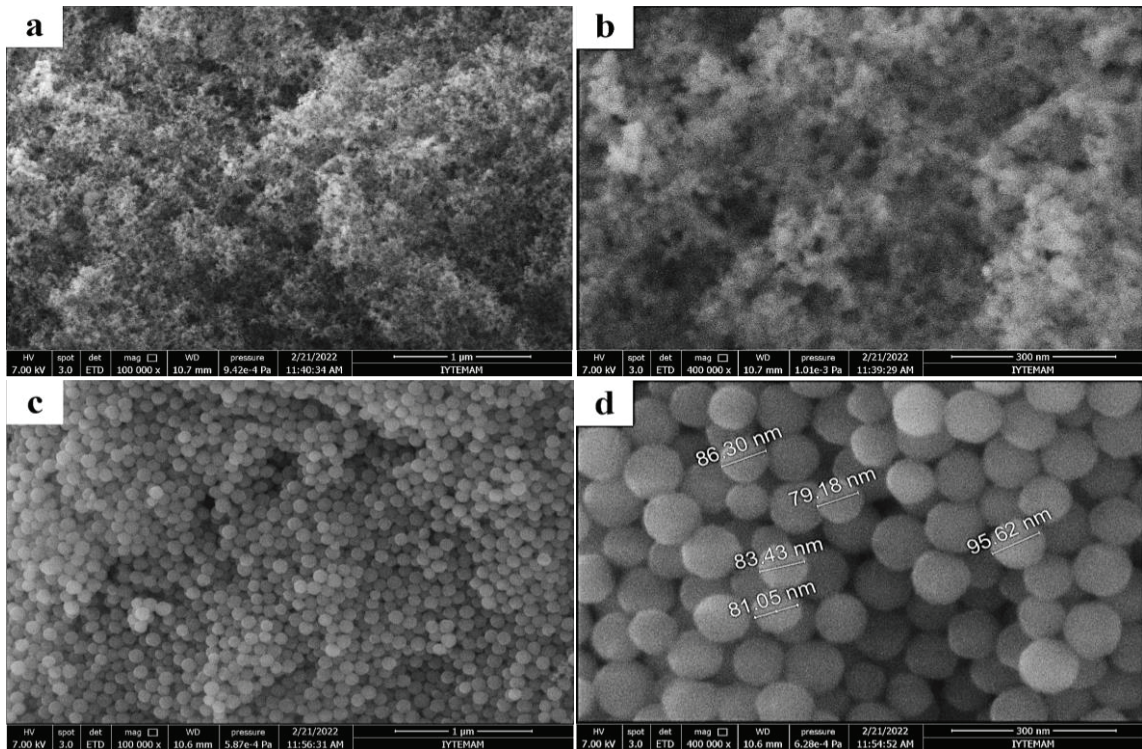
Figure 4.1 SEM images of untreated fumed silica particles (a) at a magnification of 100,000x, (b) at a magnification of 400,000x and colloidal silica particles (c) at a magnification of 100,000x, (d) at a magnification of 400,000x
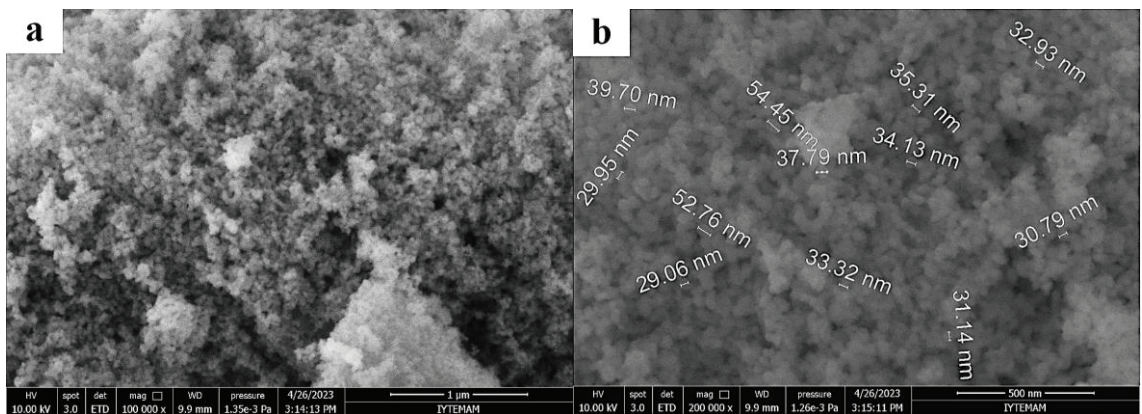
(cont. on next page)

Figure 4.2 SEM images of untreated zirconia particles (a) at a magnification of 100,000x, (b) at a magnification of 200,000x, and hydroxyapatite particles (c) at a magnification of 100,000x, (d) at a magnification of 200,000x
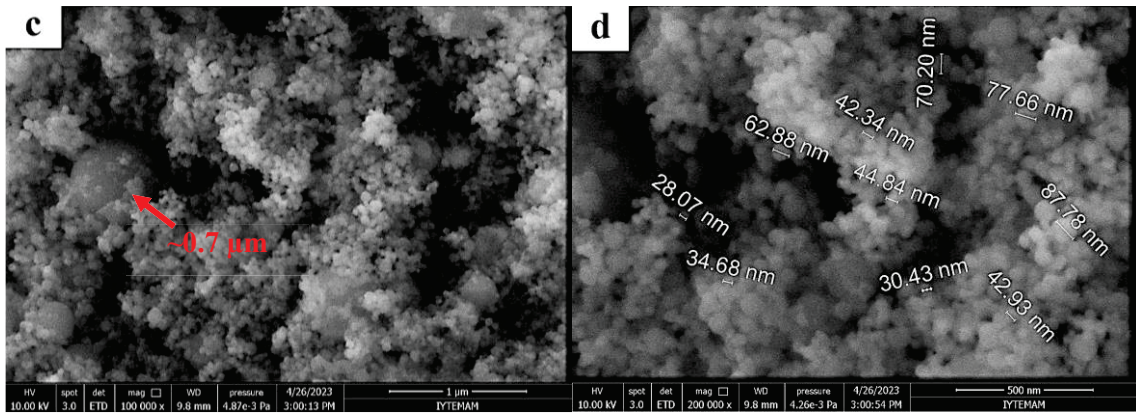
Figure 4.2 (cont.)

SEM images of modified barium glass particles at magnifications of 25,000x and 100,000x are shown in Figure 4.3 (a) and (b), respectively. The typical morphology of barium glass particles was observed from SEM images. They have an irregular shape with an average particle size of 0.7 µm.
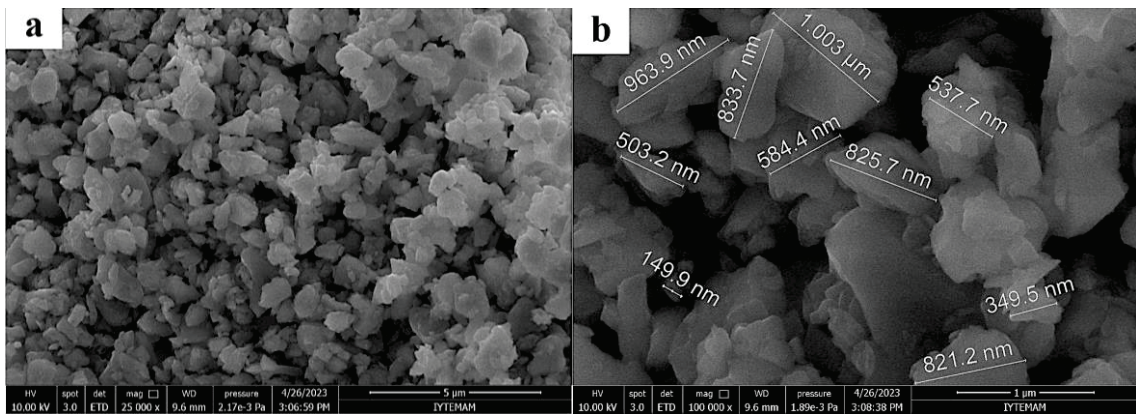
Figure 4.3 SEM images of modified barium glass particles at a magnification of (a) 25,000x and (b) 100,000x

The fracture surfaces of the samples damaged after the three-point bending test were examined by using SEM. Representative SEM images of the fracture surfaces of the composites at 1,000x magnification are given in Figure 4.4. It can be said that the fracture surface of the sample REF containing only silica and Ba glass particles is flatter compared to other composites. This implies that the sample REF exhibits poor resistance to crack

propagation and lower energy is required to break the sample. It is seen that other samples have curved and rough surfaces. Curved surfaces may be due to zirconia and HA particles deflecting crack propagation. The rough surface implies that higher fracture energy will be required to break the sample or the material can absorb higher energy during fracture. Zirconia and HA particles can increase the overall toughness of the composite by slowing the crack propagation, thanks to their high hardness. In addition, most of the samples showed a small amount of micro-voids as seen in Figure 4.4 (c) and (f). This is due to the difficulty of getting rid of bubbles during the placement of the samples into the mold.

Representative SEM images of the fracture surfaces of the composites at 10,000x magnification are given in Figure 4.5. In almost all samples, homogeneous particle distribution was observed at this magnification. Irregularly shaped and light-colored Ba glass particles also can be seen clearly in all samples.

The average HA size is known as 200 nm. However, it was stated that there are also HA particles as large as 0.7 μm, as seen in Figure 4.2 (c). Although small HA particles cannot be distinguished, it is easily understood from SEM images that the large ones are HA. It is seen that spherical shaped particles with a size of 0.5-1 μm thought to be HA particles in H3Z1 and especially in H5Z2 sample were forced out of the matrix as a result of weak interfacial bond in Figure 4.5 (f) and (i). These particles are marked in red. In other samples, it is seen that the particles are adhered to the matrix and covered.
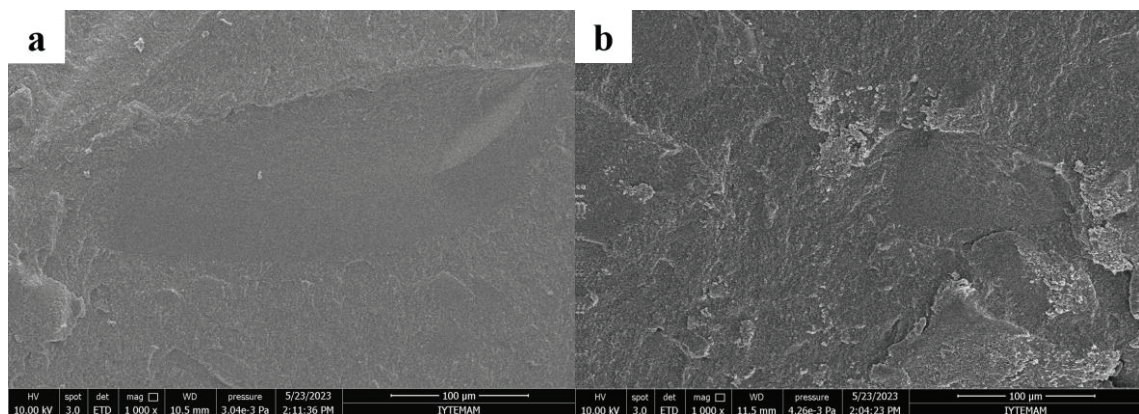
Figure 4.4 SEM images of the fracture surface of the representative dental composites at a magnification of 1,000x (a)REF, (b) H3, (c) H5, (d) Z1, (e) Z2, (f) H3Z1, (g) H3Z2, (h) H5Z1 and (i) H5Z2
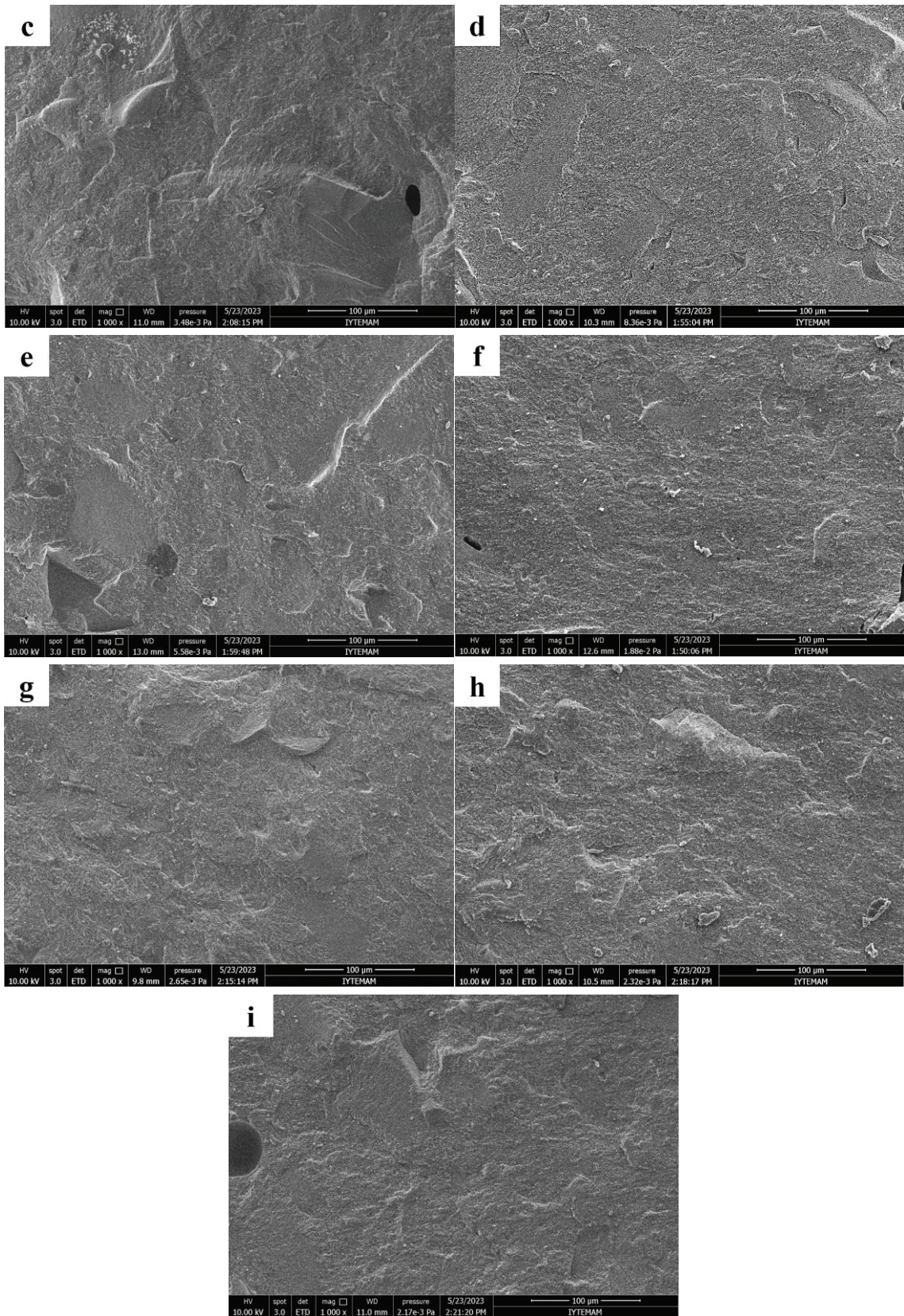
Figure 4.4 (cont.)
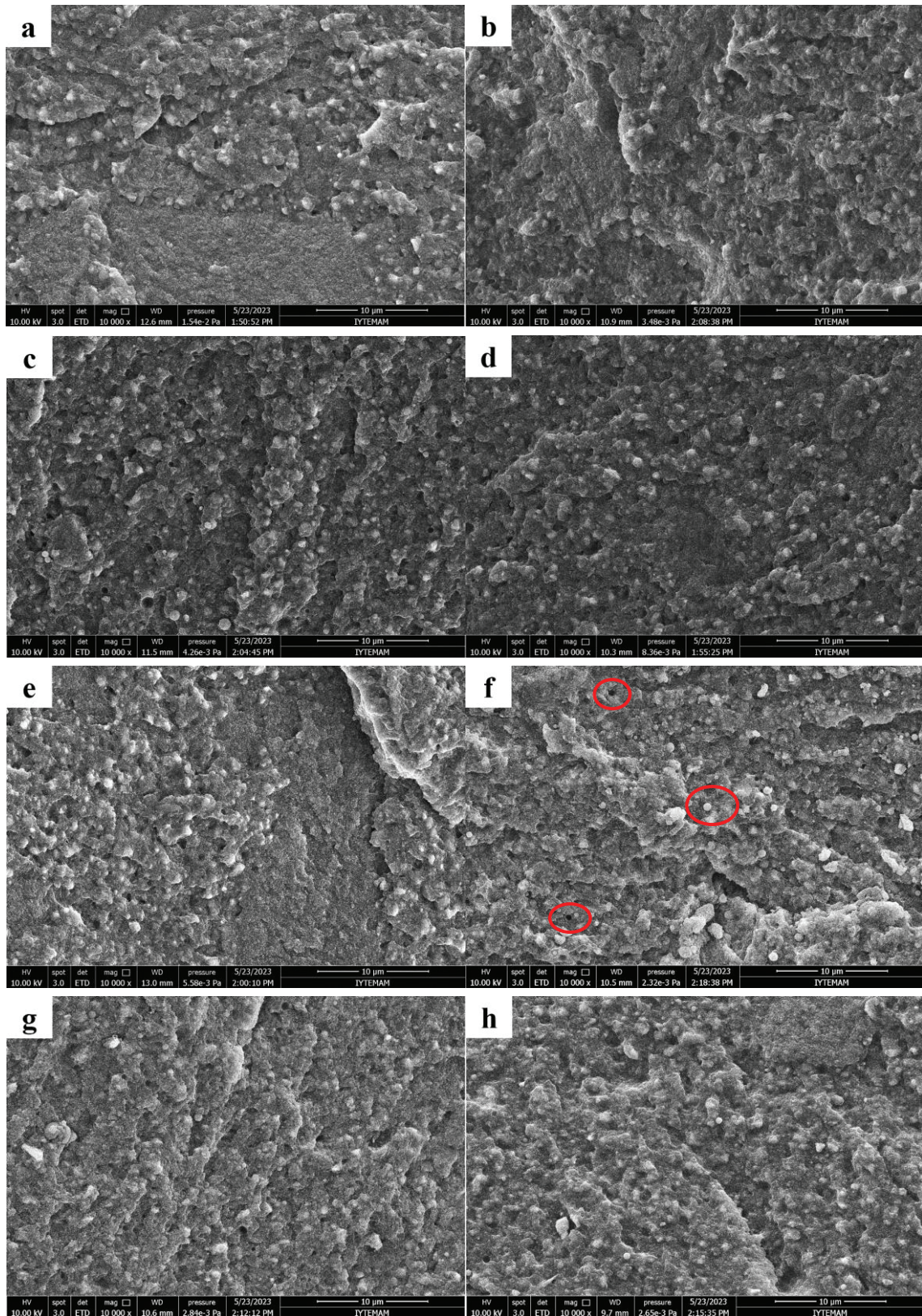
Figure 4.5 SEM images of the fracture surface of the representative dental composites at a magnification of 10,000x (a)REF, (b) H3, (c) H5, (d) Z1, (e) Z2, (f) H3Z1, (g) H3Z2, (h) H5Z1 and (i) H5Z2
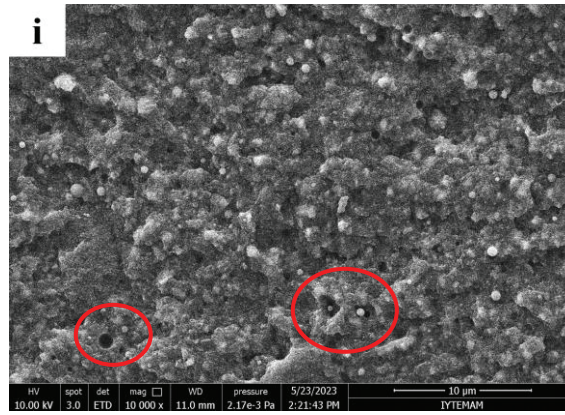
Figure 4.5 (cont.)

Representative SEM images of the fracture surfaces of sample REF, Z2, H3Z1, and H5Z1 at 100,000x magnification and sample H5Z2 at 50,000x magnification are given in Figure 4.6. Sample REF containing only silica and Ba glass particles are seen in Figure 4.6 (a). Therefore, it is obvious that the agglomerated spherical shaped particles are colloidal silica. They are also evident in SEM images of Z2 in Figure 4.6 (b). Ba glass particle embedded in the matrix is also shown with a red arrow. In Figure 4.6 (c), there are small spherical shaped particles covered with matrix in different regions. These particles are colloidal silica or HA particles and are indicated by the red arrow. Figure 4.6 (d) shows the HA particles forced out of the matrix during the mechanical test.
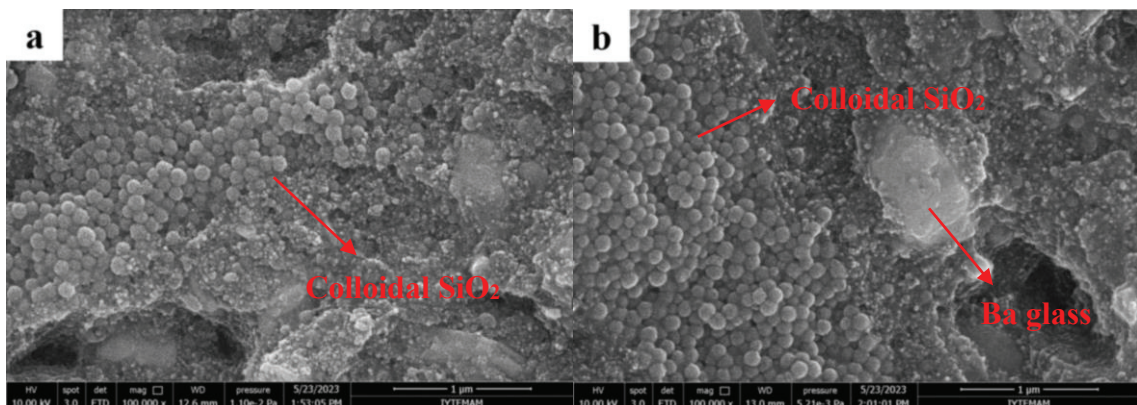
(cont. on next page)

Figure 4.6 SEM images of the fracture surface of the representative dental composites at a magnification of 100,000x (a)REF, (b) Z2, (c) H5Z1, and at a magnification of 50,000x (d) H5Z2
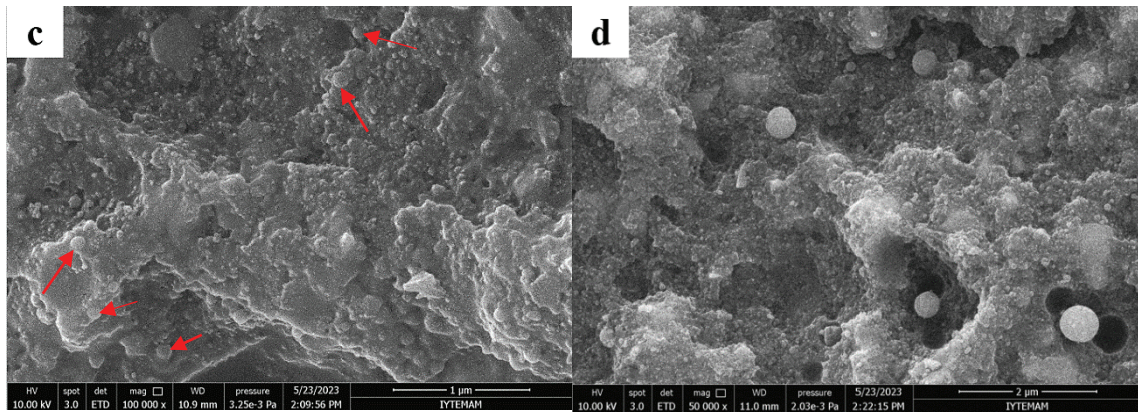
Figure 4.6 (cont.)

4.1.2 Dynamic Light Scattering (DLS)

Particle size distributions of the particles used in this study were given in Figure 4.7. The particle size of fumed silica is in the range of 70-600 nm. The reason for this wide range is the presence of large-sized particles due to the agglomeration of fumed silica particles. The particle size distributions of colloidal silica, zirconia, HA, and barium glass were found as 60-300 nm, 7-40, 130-960 nm, and 560-770 nm, respectively.
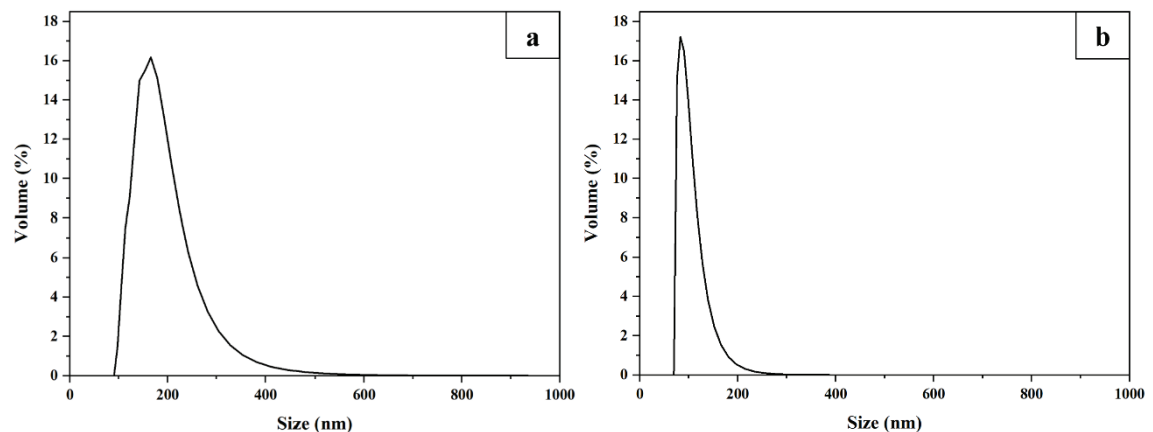
Figure 4.7 Size distributions as a function of volume % of (a) fumed silica, (b) Colloidal silica, (c) zirconia, (d) hydroxyapatite, and (d) barium glass particles
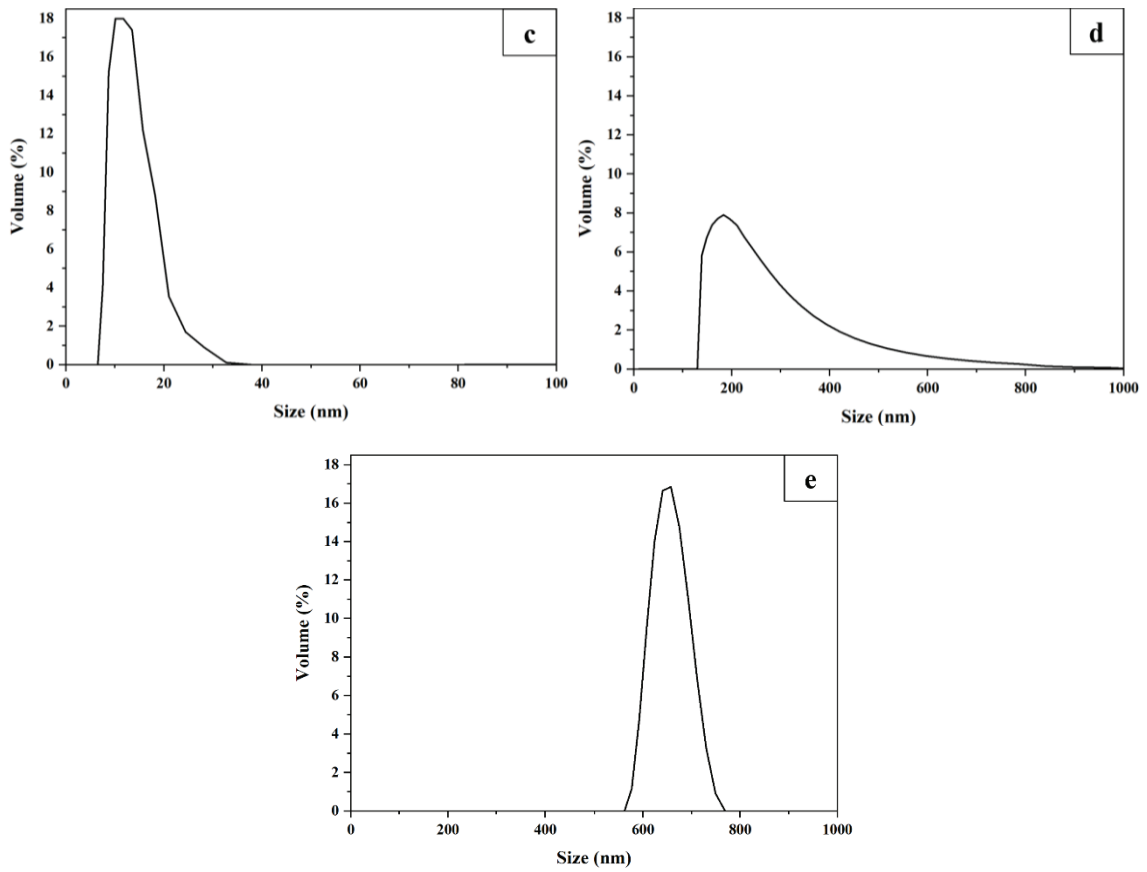
Figure 4.7 (cont.)

The average particle sizes of the particles used in this study were given in Table 4.1. Average particle sizes of fumed silica, colloidal silica, zirconia, HA, and barium glass were found as 212, 134.3, 12.99, 256.7, and 654.4 respectively.

Table 4.1 Average particle sizes of the inorganic filler particles

Inorganic Filler Type	Average Particle Size (nm)
Fumed silica	212.0
Colloidal silica	134.3
Zirconia	12.99
Hydroxyapatite	256.7
Barium glass	654.4

4.1.3 Fourier Transform Infrared Spectroscopy (FT-IR)

FTIR spectra of untreated and treated filler particles used in composites including fumed and colloidal silica, zirconia, and hydroxyapatite and barium glass which is treated as-received are given in Figure 4.8. The functional groups observed in their FTIR spectra and corresponding wavenumbers are presented in Table 4.2. A peak is seen at wavenumber 400-500 cm^{-1} in (a) and (b) is due to bending vibration of the Si–O–Si (siloxane) bond, which is present in the structure of silica and also formed after surface modification with γ-MPS (Aydınoğlu et al. 2022). The peak seen at 811 cm^{-1} indicates Si–OH bonding. This peak is due to the hydroxyl (OH) groups on the surface of the silica particles (Najafi et al. 2017). The particles showed an intense absorption band at 1100 cm^{-1}. It is due to the stretching vibration of Si–O–Si bond (Miao et al. 2012). The intensity of this peak is higher in modified particles. It indicates the formation of Si–O–Si bond thanks to the surface modification.

In Figure 4.8 (c), peaks were seen at 485 cm^{-1} and 756 cm^{-1} corresponding to the bending vibration of the Zr-O bond in the structure of zirconia. The weak peaks seen at 1150 cm^{-1} and around are due to the stretching vibration of the Zr-O-Zr bond in the zirconia crystal lattice (Rao et al. 2019).
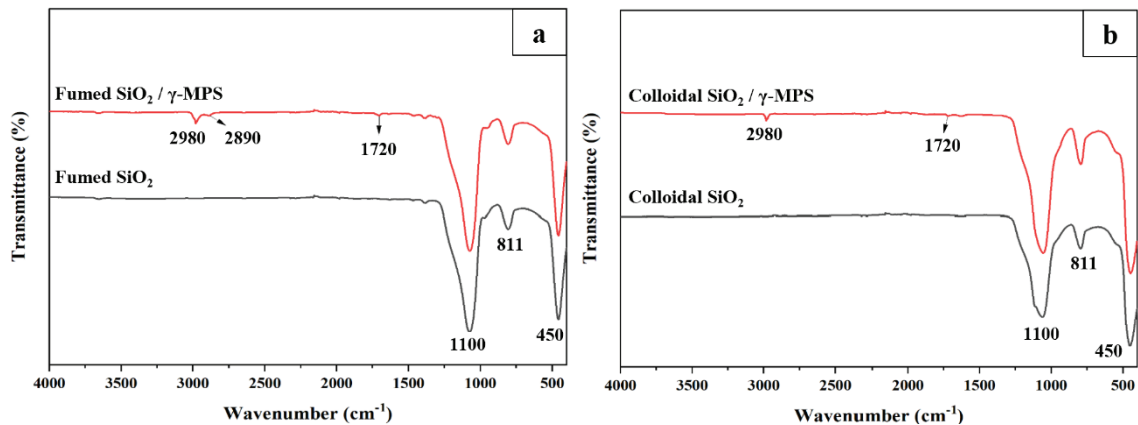
(cont. on next page)

Figure 4.8 FTIR spectra of inorganic filler particles which are untreated and treated with γ-MPS (a) fumed silica, (b) colloidal silica, (c) zirconia, (d) hydroxyapatite and (e) barium glass
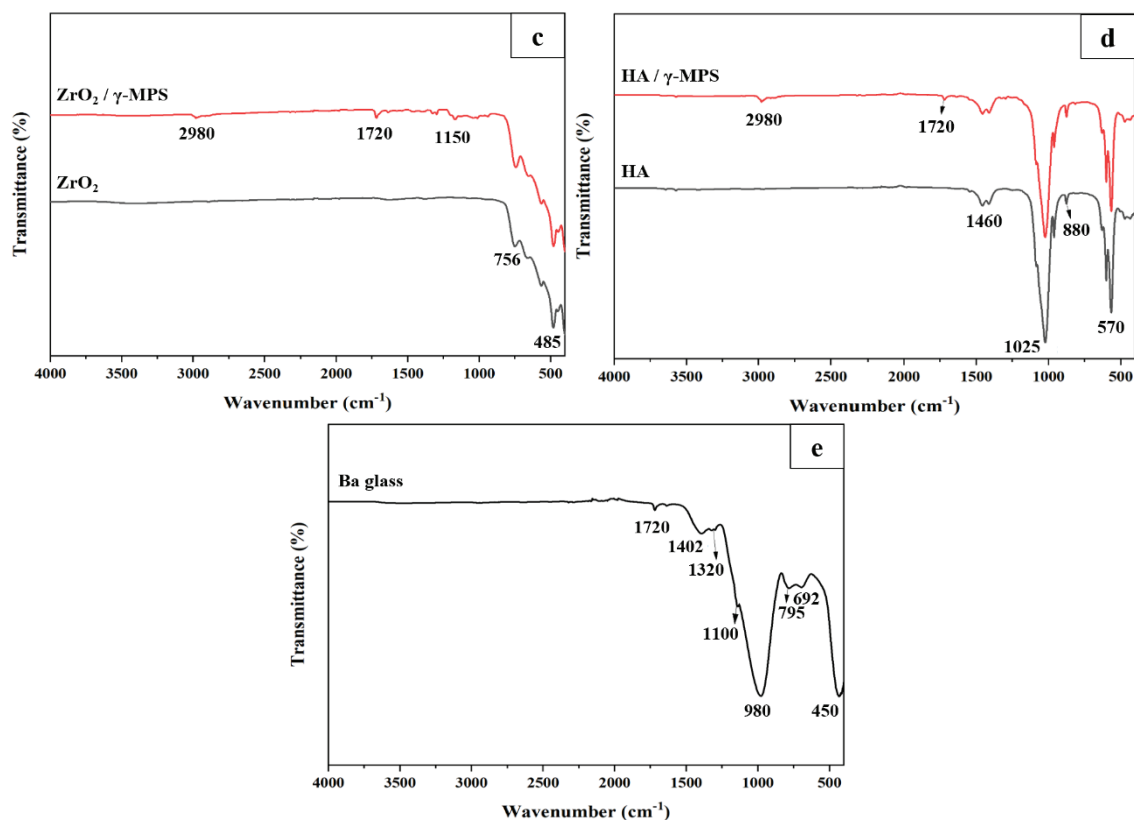
Figure 4.8 (cont.)

Table 4.2 Functional groups observed in FTIR spectra of the particles and their corresponding wavenumbers

Wavenumber (cm^{-1})	Vibration Mode	Functional Group
450	Bending	Si-O-Si
811	Bending	Si-OH
1100	Stretching	Si-O-Si
1720	Stretching	C=O
2890-2980	Stretching	C-H
485-756	Bending	Zr-O
1150	Stretching	Zr-O-Zr
570	Ion stretching	O-H
880	Asymmetric stretching	C-O
1025	Asymmetric stretching	P-O
1460	Out of plane bending	C-O
692	Bending	Ba-O
795	Symmetric stretching	O-Si-O
980	Bending	B-O
1320-1402	Symmetric stretching relaxation	B-O

59

In Figure 4.8 (d), the peaks of the bonds in the phosphate and carbonyl groups, which are characteristic of HA were seen (Gheisari, Karamian, and Abdellahi 2015). The peak seen at 570 cm^{-1} corresponds to the bending vibration of the P-O bond belonging to the PO$_4^{3-}$ functional group in the HA crystal lattice. The peak seen at 880 cm^{-1} is due to the deformation vibration of the carbonate (CO$_3$) group, which may be present in small amounts as a substitute for phosphate groups in the crystal lattice. An intense absorption band is observed at 1025 cm^{-1} due to the stretching vibration of the P-O bond in the phosphate groups. The peak at 1460 cm^{-1} indicates the stretching vibration of the carbonate (CO$_3$) group (Chandrasekaran 2013).

The peak seen at wavenumber 400-500 cm^{-1} is due to bending vibrations of the Si–O–Si bond which is present in the structure of the glass. A strong absorption seen at 692 cm^{-1} belongs to the bending vibration of Ba–O bond in the glass network (Ansari and Jahan 2021). This peak is characteristic of the presence of barium ions in the glass composition. The peak at 795 cm^{-1} is due to the symmetric stretching vibration of O-Si-O in the structure of the glass. The peaks at 1320 cm^{-1} and 1402 cm^{-1} belong to symmetric stretching relaxation of B-O band of BO$_3$ in the network of borosilicate glass. The peaks at 980 cm^{-1} and 1100 cm^{-1} are due to the bending vibration of B–O and the stretching vibration of Si–O–Si bond, respectively (Shao et al. 2015).

In all modified particles, a new peak is observed at 1720 cm^{-1}, resulting from the stretching vibration of the carbonyl (C-O) group in the γ-MPS structure. This carbonyl group can form hydrogen bonds with hydroxyl groups on the surface of silica particles. The peaks at 2890 cm^{-1} and 2970 cm^{-1} are caused by the stretching vibration of the C-H bond in the γ-MPS structure (Sideridou and Karabela 2009). The difference between the FTIR spectra of the modified and unmodified particles indicates that the surface modification process has taken place successfully.

4.2 Mechanical Test Results

Flexural and compressive strength is particularly important in dental applications, as dental composites are often used to restore teeth that have been subjected to such stresses during normal chewing and biting. It is reported that the flexural strength, flexural modulus, and compressive strength of the conventional resin-based dental composites

which are filled with hybrid inorganic fillers are in the range of 60 to 130 MPa, 3 to 10 GPa and, 150 to 250 MPa, respectively (Ilie and Hickel 2011).

4.2.1 Three-Point Bending Test Results

Force-displacement curves of the representative composites obtained from three-point bending tests are given in Figure 4.9. All curves are almost linear. The point that can be deduced from these curves is that the specimens did not show any signs of plastic deformation before fracture. This indicates that all tested composites exhibited brittle behavior. In addition, the energy required to break the sample REF is the lowest, consistent with SEM images. It can be said that the highest energy is required to break sample H5Z1.
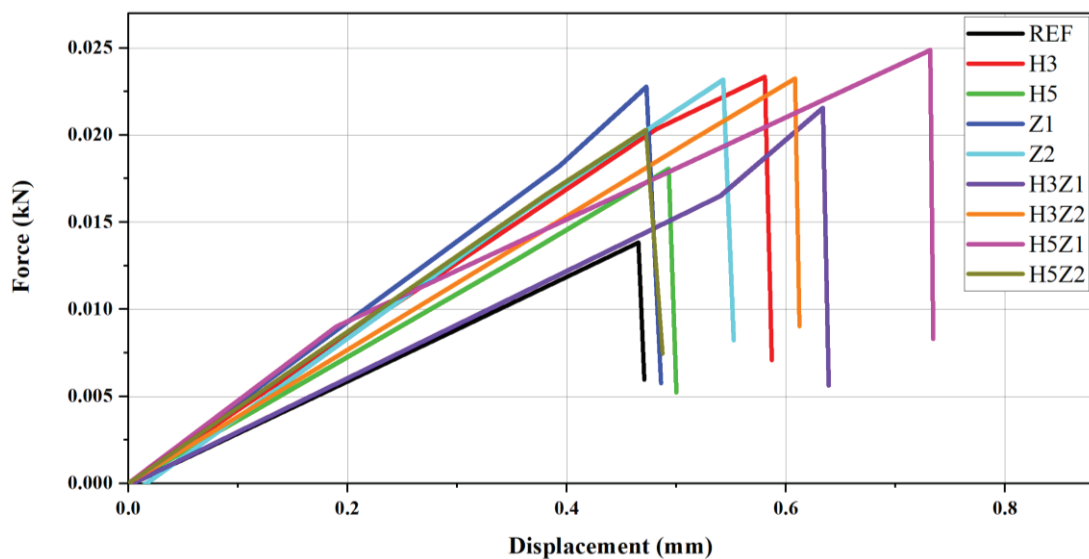
Figure 4.9 Force-displacement curves of the representative dental composites obtained from three-point bending tests

Flexural strength and flexural modulus values of the resin-based dental composites are given in Table 4.3. Flexural strength is also summarized in Figure 4.10. According to ISO 4049 standard, it is stated that the flexural strength should be a

minimum of 80 MPa for Type 1 dental materials claimed by the manufacturer to be suitable for restorations containing occlusal surfaces, while 50 MPa for all other polymer-based restorative materials. Therefore, all dental composites prepared meet the requirements of the standard and it can be said that the sample H5Z1 is in the category of Type 1 dental materials.

Table 4.3 Flexural strength and flexural modulus results of the dental composites

Sample No	Flexural Strength (MPa)	Flexural Modulus (GPa)
REF	52.17 ± 3.36	3.16 ± 0.22
H3	67.61 ± 1.93	4.21 ± 0.49
H5	73.50 ± 3.83	3.94 ± 0.41
Z1	68.39 ± 6.08	5.05 ± 0.38
Z2	71.65 ± 6.85	4.68 ± 0.62
H3Z1	72.79 ± 5.87	3.75 ± 0.61
H3Z2	75.50 ± 4.72	4.07 ± 0.19
H5Z1	82.78 ± 1.45	3.96 ± 0.61
H5Z2	75.37 ± 5.84	4.31 ± 0.34
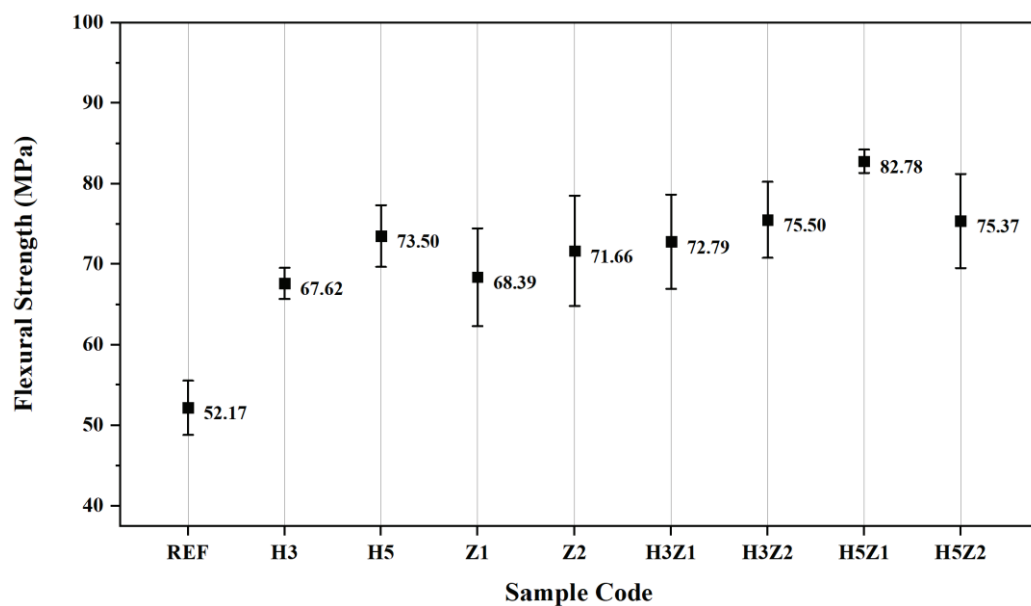
Figure 4.10 Flexural strength results of the dental composites with a standard deviation

62

The flexural strength of all samples was higher than the control sample REF. It can be said that both particle types have a reinforcing effect. The flexural strength increases with increasing zirconia and HA ratio. A greater increase was achieved in the lower addition of zirconia compared to HA.

The interaction of the two particle types is significant. There was a 9% improvement when HA was increased from 3 (sample H3) to 5 wt.% (sample H5). However, when the zirconia was kept constant at 1 wt.%, a 14% increase was achieved with increasing HA from 3 (sample H3Z1) to 5 wt.% (sample H5Z1). The highest flexural strength value was obtained in the sample H5Z1. In this sample, it is seen that the particles are well dispersed and adhered to the matrix, as seen in Figure 4.6 (c). The damage occurred in the matrix in the three-point bending test.

While the flexural strength increased with the addition of zirconia and HA, it decreased in sample H5Z2. When SEM images of the sample were examined, it was observed that some spherical HA particles have been forced out of the matrix during the mechanical testing. This is because of the weak filler/matrix interface which prevents effective stress transfer between fillers and matrix. Therefore, it has a negative effect on the flexural strength. A small increase was seen in sample H3Z1 compared to samples H3 and Z1. This may be due to displaced HA particles similar to the H5Z2 sample as seen in the SEM images.

The flexural modulus is also summarized in Figure 4.11. The flexural modulus of the conventional resin-based dental composites filled with hybrid inorganic fillers in the literature ranges from 3 to 10 GPa and commercial composites used today are usually around 10 GPa. The flexural modulus values of all samples are compatible with the literature. The flexural modulus of the samples varies in the range of 3.16-5.06. Because zirconia and HA particles have a higher modulus than the polymer matrix, all samples have a higher flexural modulus than the control sample REF. The presence of particles in the matrix provides an increase in modulus by limiting the movement of the matrix phases surrounding the particles.

HA particles have a small effect on the flexural modulus. On the other hand, with the increase in the amount of zirconia, there is an increase in the flexural modulus of all samples. The highest modulus was obtained in the sample Z2. This is because the hard and rigid zirconia nanoparticles resist deformation under load, which increases the overall stiffness of the material.
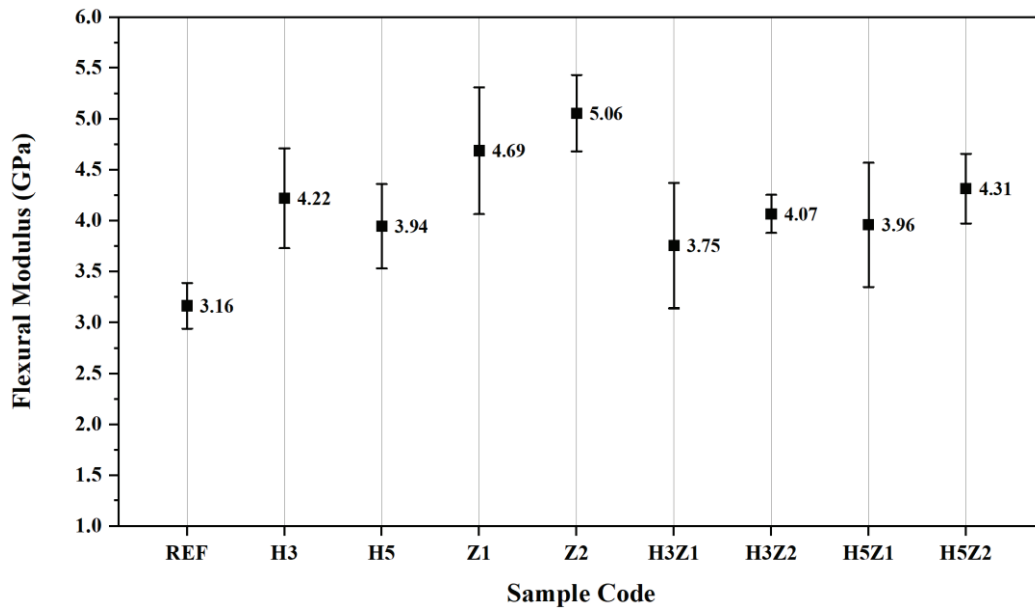
Figure 4.11 Flexural modulus results of the dental composites with a standard deviation

4.2.2 Compression Test Results

Force-displacement curves of the representative composites obtained from compression tests are given in Figure 4.12. All curves are almost linear, as are the curves obtained from the three-point bending test. It can be also said that the specimens did not show any signs of plastic deformation before fracture. This indicates that all tested composites showed brittle behavior. The energy required to break the sample REF is the lowest again.

The compression test results of the composites prepared are given in Table 4.4 and Figure 4.13. The compressive strength of the conventional resin-based dental composites filled with hybrid inorganic fillers in the literature ranges from 150 to 250 MPa. Compression test results of all samples are compatible with the literature. All samples except sample H5Z2 have higher compressive strength than the control sample REF.

The packing density of zirconia and HA particles increased with the increasing filler loading, thereby improving the compressive strength. A greater increase was achieved with the increasing addition of HA compared to zirconia. Although the sample H3Z1 shows higher compressive strength compared to sample H3 and Z1, it has a lower value than samples H5 and Z2. It is also seen that the standard deviation is high. This may be

due to the undesirable distribution of the particles. The highest compressive strength value is obtained in sample H3Z2 and then it started to decrease.
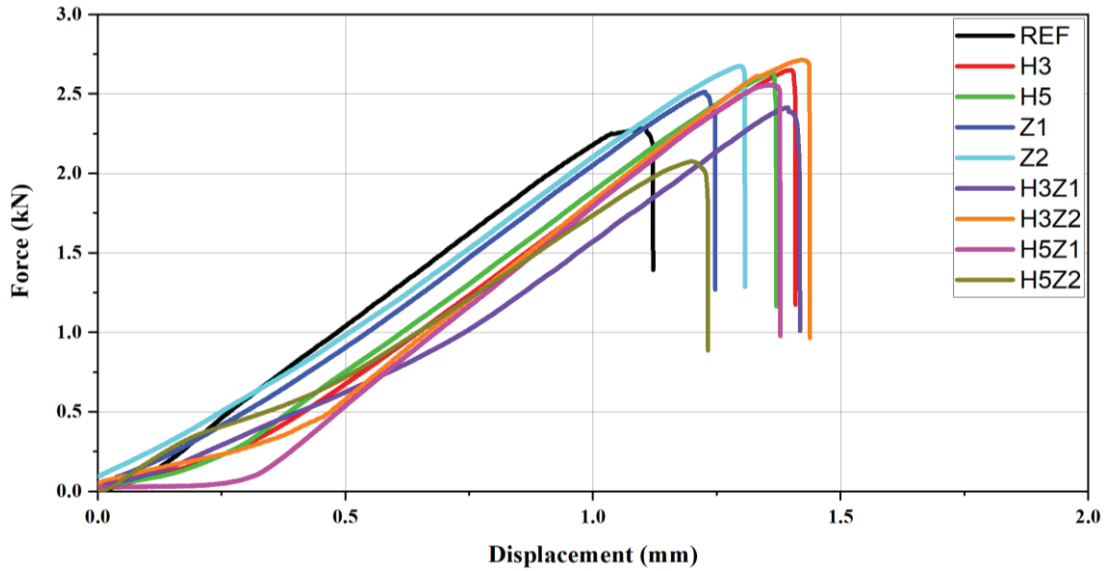
Figure 4.12 Force-displacement curves of the representative dental composites obtained from compression tests

Table 4.4 Compressive strength results of the dental composites

Sample No	Compressive Strength (MPa)
REF	183.15 ± 9.15
H3	208.40 ± 7.78
H5	213.12 ± 13.45
Z1	206.66 ± 12.57
Z2	212.72 ± 6.82
H3Z1	209.19 ± 16.05
H3Z2	222.63 ± 6.40
H5Z1	209.66 ± 6.31
H5Z2	178.49 ± 6.38

When zirconia was added alone, the compressive strength increased by approximately 3% by increasing its amount from 1 wt.% to 2 wt.%. However, while the

amount of HA was kept at 3 wt.%, increasing the amount of zirconia from 1 wt.% to 2 wt.% increased the compressive strength by 6%. It can be said that they have a synergistic effect.
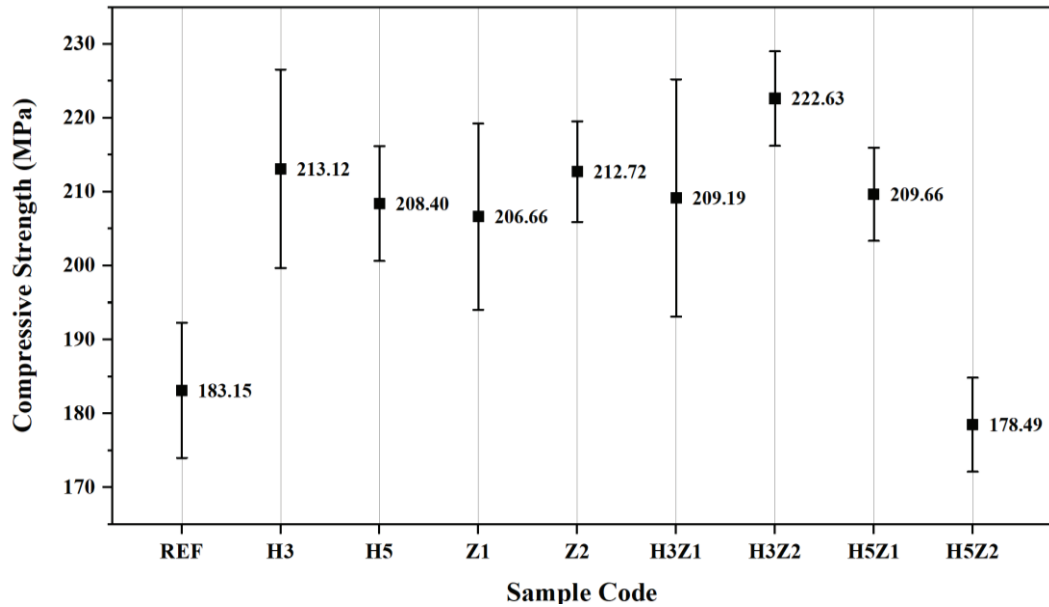
Figure 4.13 Compressive strength results of the dental composites with a standard deviation

Since the compression test specimens have a height of 6 mm, it can be said that there is a relationship between the compressive strength and depth of cure, which is given in Table 4.5. In samples H5Z1 and H5Z2, with the increase of HA and especially zirconia particles, the refractive index of which is much higher than the resin, the depth of cure decreased and thus the compressive strength decreased. In addition, it can be said that HA particles with a weak interface have an adverse effect on the compressive strength of the sample H5Z2.

4.3 Depth of Cure Examination Results

The depth of cure of the prepared resin-based dental composites with standard deviation is given in Table 4.5 and Figure 4.14, respectively. According to ISO 4049

standard, all samples meet the limit value for a depth of cure of 1.5 mm. The highest value was seen in sample REF, while H5Z2 showed the lowest depth of cure. It is seen that the depth of cure decreases with increasing amount of zirconia and HA filler loading. It can be said that an increase in zirconia amount causes a greater decrease in the depth of cure compared to HA.

Table 4.5 Depth of cure values of the dental composites

Sample No	Depth of Cure (mm)
REF	2.99 ± 0.05
H3	2.85 ± 0.07
H5	2.75 ± 0.08
Z1	2.59 ± 0.04
Z2	2.35 ± 0.04
H3Z1	2.50 ± 0.03
H3Z2	2.40 ± 0.05
H5Z1	2.47 ± 0.05
H5Z2	2.07 ± 0.06

Light transmittance is the main factor affecting the depth of cure. Resin is an organic matrix that is transparent to visible light, while inorganic filler particles cause light scattering. For the light transmittance to be high, the refractive index of the particles should be similar to that of the resin, so that scattering is reduced. The refractive index of the resins and filler particles used in this study are given in Table 2.5. The refractive index of the three monomers and silica used is very close to each other. On the other hand, the indices of HA and especially zirconia are much higher than that of the resin. This results in the scattering of light and a reduction in the depth of cure. Wang et al. also reported that zirconia particles significantly reduced light transmission into the deep layers of the composite (Wang et al. 2020).
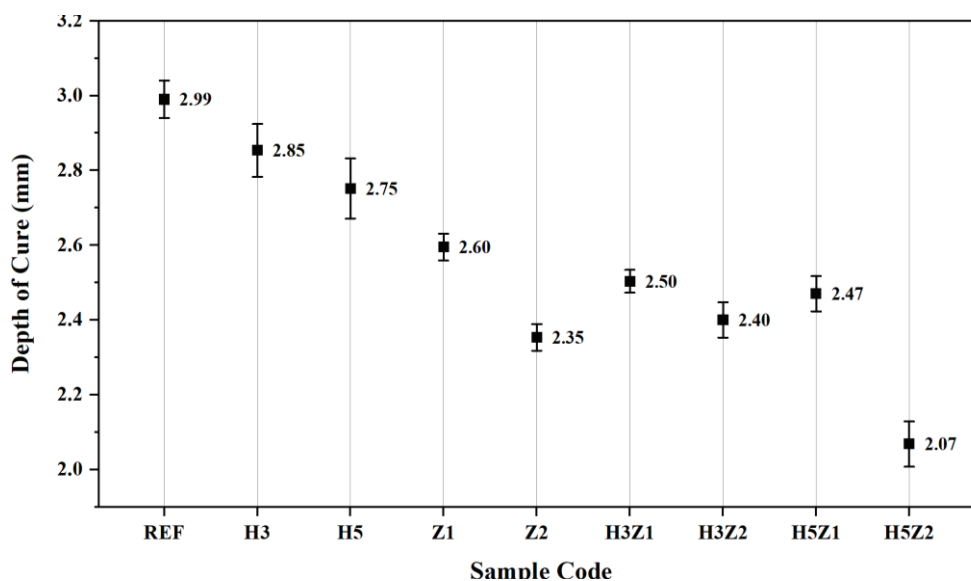
Figure 4.14 Depth of cure values of the dental composites with a standard deviation

4.4 Water Sorption and Solubility Test Results

Because dental composites are used in the mouth, they are exposed to saliva or other fluids. Water has an important role in the deterioration of these composites and their clinical lifetime. Therefore, water sorption and solubility properties of composites should be evaluated (Al Badr 2018). Water sorption and solubility results are given in Table 4.6 and Figure 4.15.

Table 4.6 Water sorption and solubility results of the dental composites

Sample No	Water Sorption ($\mu g/mm^3$)	Water Solubility ($\mu g/mm^3$)
REF	12.32 ± 0.72	0.53 ± 0.32
H3	13.03 ± 1.21	1.19 ± 0.30
H5	14.27 ± 1.14	1.20 ± 0.41
Z1	12.26 ± 1.26	0.54 ± 0.22
Z2	12.88 ± 1.13	0.78 ± 0.19
H3Z1	12.61 ± 0.68	0.98 ± 0.66
H3Z2	12.97 ± 1.24	1.55 ± 0.57
H5Z1	12.51 ± 0.48	0.81 ± 0.38
H5Z2	14.26 ± 1.34	1.63 ± 0.95
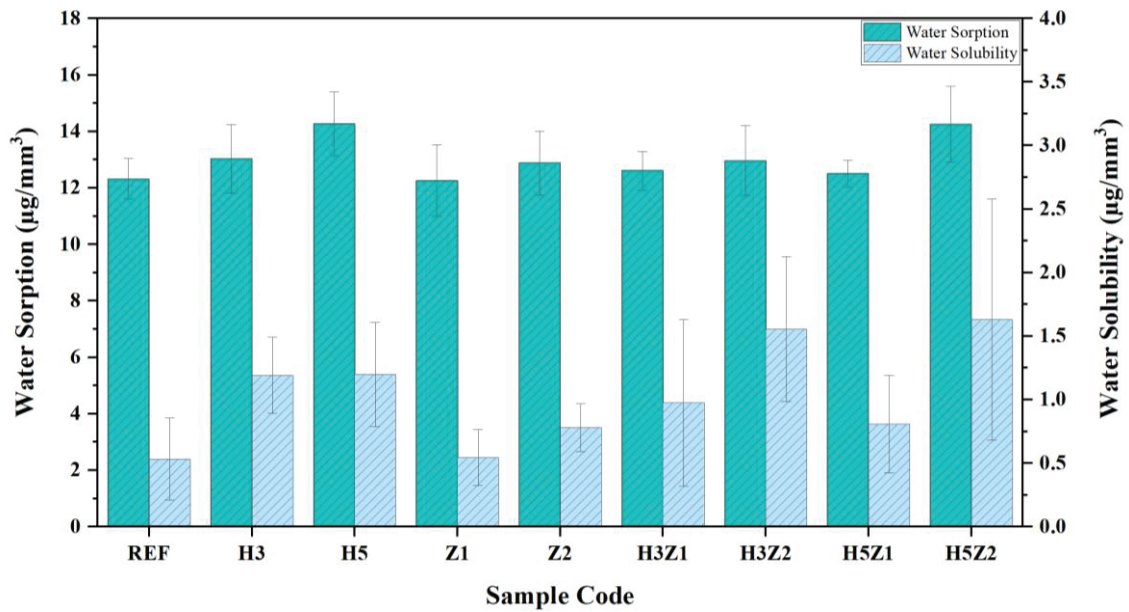
Figure 4.15 Water sorption and solubility results of the dental composites with a standard deviation

According to ISO 4049 standard, water sorption should be equal to or less than 40 $\mu g/mm^3$ and solubility should be equal to or less than 7.5 $\mu g/mm^3$. All composites have low water sorption and solubility values and meet the requirements of ISO 4049 standards.

Sample REF containing only silica and Ba glass particles showed the lowest water sorption. Water sorption increases with the addition of zirconia and HA. Thanks to the hydroxyl groups on the surface of silica particles, silica provides a more efficient surface modification compared to other particles (Habib et al. 2016). This resulted in a stronger interface between the particle and the matrix, preventing water sorption from the interface.

Since zirconia nanoparticles provide a larger surface area, water diffusion between the particles and the matrix is facilitated, and water sorption and solubility values increased (Al Badr 2018). It can be said that HA particles increased water sorption more than zirconia nanoparticles. This may be due to the hydrophilic nature of HA particles.

The highest water sorption values were observed in samples H5 and H5Z2. This can be attributed to the presence of micro-voids in sample H5 and the poor interface between HA particles and the matrix in sample H5Z2, as seen in Figure 4.4 (c) and Figure 4.6 (d), respectively.

There is an almost linear relationship between water sorption and solubility. Because water penetrating the composite causes unreacted monomers and decomposed components to come out of the composite (Liu, Jiang, et al. 2014). The degree of conversion is also an important factor affecting the water solubility of the composite. If the degree of conversion of the prepared composites is analyzed, the solubility values can be clearly explained (Domingo et al. 2001; El-Banna, Sherief, and Fawzy 2019).

CHAPTER 5

CONCLUDING REMARKS

The main problem with resin-based dental composites is failure due to fracture and secondary caries, which compromises long-term durability in clinical use. In order to overcome these problems, the mechanical properties and water sorption and solubility properties of the composite must be improved. Many studies have been carried out with combinations of different monomer and inorganic filler particles to achieve it. In particular, it is reported that the type and amount of inorganic particles used have a critical effect on the mechanical properties of the composite. In this study, single and cross effects of zirconia, which is known to improve the mechanical and aesthetic properties of the composite, and hydroxyapatite nanoparticles, which are present in the structure of the tooth and preferred due to their biological and mechanical properties, on the properties of the composite were investigated. It is aimed to improve the mechanical properties of the composite, as well as water sorption and solubility properties. In this study, optimum properties were obtained in the sample H5Z1.

Different amounts of addition were determined as 3 and 5 wt.% for hydroxyapatite and 1 and 2 wt.% for zirconia nanoparticles according to the literature. The flexural strength and flexural modulus, compressive strength, depth of cure, water sorption and solubility properties of the prepared composites were investigated. Samples were characterized using Scanning Electron Microscopy (SEM) and Fourier Transform Infrared Spectroscopy (FTIR).

The surface modification of γ-MPS treated particles was examined by performing FTIR analysis. The difference between FTIR spectra of the untreated and treated particles indicates that the surface modification process has been carried out successfully. In SEM images, it is seen that the particles adhere well to the matrix and the composites are prepared successfully. In samples H3Z1 and H5Z2, it is seen that some 0.5-1 μm spherical shaped particles, which are thought to be HA particles, were forced out of the matrix as a result of weak interfacial bonding.

The mechanical properties of all composites meet the requirements of ISO 4049 standard. The force-displacement curves of representative composites obtained from

three-point bending and compression tests are nearly linear. It can be deduced from these curves that the samples did not show any signs of plastic deformation before fracture. This indicates that all tested composites exhibited brittle behavior.

Zirconia and HA particles showed significant improvement in the flexural and compressive strength of the composites. The highest flexural strength was obtained in sample H5Z1 and an increase of 58% was achieved compared to the sample REF. The highest compressive strength was obtained in the sample H3Z2, and an increase of 22% was achieved compared to the sample REF.

According to ISO 4049 standard, all composites meet the depth of cure limit value of 1.5 mm. The highest value was seen in the sample REF, while H5Z2 showed the lowest depth of cure. It is seen that the depth of cure decreases with increasing amount of zirconia and HA filler loading. The refractive index of the three monomers and silica is very close to each other. On the other hand, the indices of HA and especially zirconia are much higher than that of resin. This results in scattering of light and reduced depth of cure.

All composites have low water sorption and solubility values and meet the requirements of ISO 4049 standard. Sample REF containing only silica nanoparticles showed the lowest water sorption. Water sorption increases with the addition of zirconia and HA. Since zirconia nanoparticles have a larger surface area, water diffusion between the particles and the matrix is facilitated, and water sorption and solubility values increase. The highest water sorption values were observed in samples H5 and H5Z2. This can be attributed to the presence of micro-voids in sample H5 and the poor interface between HA particles and the matrix in sample H5Z2.

5.1 Future Works

It can be said that zirconia and HA nanoparticles have a synergistic effect. The combined use of these nanoparticles is promising in terms of mechanical properties and water sorption and solubility properties. However, there are other characteristics that must be met before it can be used as a commercial product. In addition, there are numerous significant questions that still need to be answered from a research perspective. Some of these topics that are worthy of further exploration are listed below.

- It has been reported that HA particles inhibit biofilm formation. Because it is significant in terms of preventing secondary caries, antibacterial properties of the composites prepared should be evaluated by performing a cytotoxicity test.

- High degree of conversion is an essential material property to achieve optimum physical and mechanical properties. The degree of conversion should be determined by analyzing the composites with FT-IR. The ratio of the height of aliphatic and aromatic C=C peak absorption at $1637cm^{-1}$ and $1580 cm^{-1}$, respectively, in the spectra of the composites before and after curing is calculated.

- Resin-based dental composites experience volumetric shrinkage of approximately 2-6% during polymerization. The bonding of composites to the tooth structure limits the strain that the material can withstand, so shrinkage leads to stresses. These stresses result in restoration fractures. In addition, marginal leakage may occur due to shrinkage and secondary caries may occur. In this case, clinical failure of the restoration takes place again. The effects of zirconia and HA nanoparticles on the polymerization shrinkage should be evaluated.

- It was observed that some large-sized HA particles were forced out of the matrix. It has negatively affected the flexural strength of the composite. Efforts should be made to increase the efficiency of the surface modification process and thus obtain a stronger interface.

- The distribution of particles is the main factor controlling the properties of resin-based dental composites. In this study, some colloidal silica particles were found to be agglomerated. Therefore, the distribution should be improved.

- Effect of particles size on the properties of resin-based dental composites also can be investigated.

REFERENCES

Amdjadi, Parisa, Amir Ghasemi, Farhood Najafi, and Hanieh Nojehdehian. 2017. "Pivotal Role of Filler/Matrix Interface in Dental Composites: Review." *Biomedical Research (India)*.

Ansari, Manauwar Ali, and Nusrat Jahan. 2021. "Structural and Optical Properties of BaO Nanoparticles Synthesized by Facile Co-Precipitation Method." *Materials Highlights* 2 (1–2): 23. https://doi.org/10.2991/mathi.k.210226.001.

Aydınoğlu, Aysu, Jülide Hazal Türkcan, Ergün Keleşoğlu, and Afife Binnaz Hazar Yoruç. 2022. "Development of Biomimetic Hydroxyapatite Containing Dental Restorative Composites." *Arabian Journal for Science and Engineering* 47 (5): 6667–78. https://doi.org/10.1007/s13369-022-06648-1.

Badr, Rafid M Al. 2018. "Effect of Addition ZrO 2 Nanoparticles to Dental Composites on the Physical and Mechanical Properties." *International Journal of Scientific & Engineering Research* 9 (6). http://www.ijser.org.

Bapat, Ranjeet A., Ho Jan Yang, Tanay V. Chaubal, Suyog Dharmadhikari, Anshad Mohamed Abdulla, Suraj Arora, Swati Rawal, and Prashant Kesharwani. 2022. "Review on Synthesis, Properties and Multifarious Therapeutic Applications of Nanostructured Zirconia in Dentistry." *RSC Advances*. Royal Society of Chemistry. https://doi.org/10.1039/d2ra00006g.

Barszczewska-Rybarek, Izabela Maria. 2019. "A Guide through the Dental Dimethacrylate Polymer Network Structural Characterization and Interpretation of Physico-Mechanical Properties." *Materials* 12 (24). https://doi.org/10.3390/MA12244057.

Byrne, Gregory S. 1984. "Adhesive Formulations Manipulated by the Addition of Fumed Colloidal Silica." *Studies in Conservation* 29: 78–80. https://doi.org/10.1179/sic.1984.29.Supplement-1.78.

Chan, K. S., D. P. Nicolella, B. R. Furman, S. T. Wellinghoff, H. R. Rawls, and S. E. Pratsinis. 2009. "Fracture Toughness of Zirconia Nanoparticle-Filled Dental Composites." *Journal of Materials Science* 44 (22): 6117–24. https://doi.org/10.1007/s10853-009-3846-4.

Chandrasekaran, Arunseshan. 2013. "Synthesis and Characterization of Nano-Hydroxyapatite (n-HAP) Using the Wet Chemical Technique Synthesis and Characterization of Yttrium Stabilized Zirconia Nanoparticles View Project Study on Electrical, Magnetic and Gas Sensing Properties of Doped TiO2 Nanoparticles and Nanotubes View Project." *Article in International Journal of Physical Sciences*. https://doi.org/10.5897/IJPS2013.3990.

Chaughule, Ramesh S. 2018. *Dental Applications of Nanotechnology*. *Dental Applications of Nanotechnology*. https://doi.org/10.1007/978-3-319-97634-1.

Chen, Hongyan, Ruili Wang, Jiadong Zhang, Hongfei Hua, and Meifang Zhu. 2018. "Synthesis of Core-Shell Structured ZnO@m-SiO2 with Excellent Reinforcing Effect and Antimicrobial Activity for Dental Resin Composites." *Dental Materials* 34 (12): 1846–55. https://doi.org/10.1016/j.dental.2018.10.002.

Chen, Liang, Qingsong Yu, Yong Wang, and Hao Li. 2011. "BisGMA/TEGDMA Dental Composite Containing High Aspect-Ratio Hydroxyapatite Nanofibers." *Dental Materials* 27 (11): 1187–95. https://doi.org/10.1016/j.dental.2011.08.403.

Cosola, Andrea, Annalisa Chiappone, Cinzia Martinengo, Hansjörg Grützmacher, and Marco Sangermano. 2019. "Gelatin Type A from Porcine Skin Used as Co-Initiator in a Radical Photo-Initiating System." *Polymers* 11 (11). https://doi.org/10.3390/polym11111901.

Cramer, N. B., J. W. Stansbury, and C. N. Bowman. 2011. "Recent Advances and Developments in Composite Dental Restorative Materials." *Journal of Dental Research* 90 (4): 402–16. https://doi.org/10.1177/0022034510381263.

Domingo, C., R. W. Arcs, A. Lpez-Macipe, R. Osorio, R. Rodrguez-Clemente, J. Murtra, M. A. Fanovich, and M. Toledano. 2001. "Dental Composites Reinforced with Hydroxyapatite: Mechanical Behavior and Absorption/Elution Characteristics." *Journal of Biomedical Materials Research* 56 (2): 297–305. https://doi.org/10.1002/1097-4636(200108)56:2<297::AID-JBM1098>3.0.CO;2-S.

El-Banna, Ahmed, Dalia Sherief, and Amr S. Fawzy. 2019. *Resin-Based Dental Composites for Tooth Filling. Advanced Dental Biomaterials*. Elsevier Ltd. https://doi.org/10.1016/b978-0-08-102476-8.00007-4.

Elfakhri, Farah, Rawan Alkahtani, Chunchun Li, and Jibran Khaliq. 2022. "Influence of Filler Characteristics on the Performance of Dental Composites: A Comprehensive Review." *Ceramics International*. Elsevier Ltd. https://doi.org/10.1016/j.ceramint.2022.06.314.

Ertl, Kathrin, Alexandra Graf, David Watts, and Andreas Schedle. 2010. "Stickiness of Dental Resin Composite Materials to Steel, Dentin and Bonded Dentin." *Dental Materials* 26 (1): 59–66. https://doi.org/10.1016/j.dental.2009.08.006.

Ferracane, J. L., T. J. Hilton, J. W. Stansbury, D. C. Watts, N. Silikas, N. Ilie, S. Heintze, M. Cadenaro, and R. Hickel. 2017. "Academy of Dental Materials Guidance—Resin Composites: Part II—Technique Sensitivity (Handling, Polymerization, Dimensional Changes)." *Dental Materials* 33 (11): 1171–91. https://doi.org/10.1016/j.dental.2017.08.188.

Ferracane, Jack L. 2011. "Resin Composite - State of the Art." *Dental Materials* 27 (1): 29–38. https://doi.org/10.1016/j.dental.2010.10.020.

Gheisari, Hassan, Ebrahim Karamian, and Majid Abdellahi. 2015. "A Novel Hydroxyapatite -Hardystonite Nanocomposite Ceramic." *Ceramics International* 41 (4): 5967–75. https://doi.org/10.1016/j.ceramint.2015.01.033.

Habib, Eric, Ruili Wang, Yazi Wang, Meifang Zhu, and X. X. Zhu. 2016. "Inorganic Fillers for Dental Resin Composites: Present and Future." *ACS Biomaterials Science and Engineering* 2 (1): 1–11. https://doi.org/10.1021/acsbiomaterials.5b00401.

Hambire, U V, and V K Tripathi. 2014. "Optimization of Compressive Strength of Zirconia Based Dental Composites." *Bull. Mater. Sci*. Vol. 37.

Heintze, Siegward D., and Brigitte Zimmerli. 2011. "Relevance of in Vitro Tests of Adhesive and Composite Dental Materials. A Review in 3 Parts. Part 3: In Vitro Tests of Adhesive Systems." *Schweizer Monatsschrift Für Zahnmedizin = Revue Mensuelle Suisse d'odonto-Stomatologie = Rivista Mensile Svizzera Di Odontologia e Stomatologia / SSO* 121 (11): 1024–40.

Hu, Cheng, Jianxun Sun, Cheng Long, Lina Wu, Changchun Zhou, and Xingdong Zhang. 2019. "Synthesis of Nano Zirconium Oxide and Its Application in Dentistry." *Nanotechnology Reviews* 8 (1): 396–404. https://doi.org/10.1515/ntrev-2019-0035.

Hyde, Emily D.E.R., Ahmad Seyfaee, Frances Neville, and Roberto Moreno-Atanasio. 2016. "Colloidal Silica Particle Synthesis and Future Industrial Manufacturing Pathways: A Review." *Industrial and Engineering Chemistry Research*. American Chemical Society. https://doi.org/10.1021/acs.iecr.6b01839.

Ilie, N., and R. Hickel. 2011. "Resin Composite Restorative Materials." *Australian Dental Journal* 56 (SUPPL. 1): 59–66. https://doi.org/10.1111/j.1834-7819.2010.01296.x.

Jin Chun, Keyoung, Choong Yeon Kim, and Jong Yeop Lee. 2016. "Mechanical Behaviors of Enamel, Dentin, and Dental Restorative Materials by Three-Point Bending Test." *Dental, Oral and Craniofacial Research* 2 (4). https://doi.org/10.15761/docr.1000167.

Kaleem, Muhammad, Julian D. Satterthwaite, and David C. Watts. 2009. "Effect of Filler Particle Size and Morphology on Force/Work Parameters for Stickiness of Unset Resin-Composites." *Dental Materials* 25 (12): 1585–92. https://doi.org/10.1016/j.dental.2009.08.002.

Kantharia, Nidhi, Sonali Naik, Sanjay Apte, Mohit Kheur, Supriya Kheur, and Bharat Kale. 2014. "Nano-Hydroxyapatite and Its Contemporary Applications." *Journal of Dental Research and Scientific Development |*. www.iadrsd.org.

Karabela, Maria M., and Irini D. Sideridou. 2008. "Effect of the Structure of Silane Coupling Agent on Sorption Characteristics of Solvents by Dental Resin-Nanocomposites." *Dental Materials* 24 (12): 1631–39. https://doi.org/10.1016/j.dental.2008.02.021.

Khaje, S, and M Jamshidi. 2015. "The Effect of Aging and Silanization on the Mechanical Properties of Fumed Silica-Based Dental Composit." *Journal of Dental Biomaterials*. Vol. 2.

Khurshid, Zohaib, Muhammad Zafar, Saad Qasim, Sana Shahab, Mustafa Naseem, and Ammar AbuReqaiba. 2015. "Advances in Nanotechnology for Restorative Dentistry." *Materials* 8 (2): 717–31. https://doi.org/10.3390/ma8020717.

Kleverlaan, Cornelis J., and Albert J. Feilzer. 2005. "Polymerization Shrinkage and Contraction Stress of Dental Resin Composites." *Dental Materials* 21 (12): 1150–57. https://doi.org/10.1016/j.dental.2005.02.004.

Kwon, Tae Yub, Rafat Bagheri, Young K. Kim, Kyo Han Kim, and Michael F. Burrow. 2012. "Cure Mechanisms in Materials for Use in Esthetic Dentistry." *Journal of Investigative and Clinical Dentistry* 3 (1): 3–16. https://doi.org/10.1111/j.2041-1626.2012.00114.x.

Labella, R, M Braden, and S Debt. 1994. "Novel Hydroxyapatite-Based Dental Composites." *Biomaterials*. Vol. 15.

Lezaja, Maja, Djordje N. Veljovic, Bojan M. Jokic, Ivana Cvijovic-Alagic, Milorad M. Zrilic, and Vesna Miletic. 2013. "Effect of Hydroxyapatite Spheres, Whiskers, and Nanoparticles on Mechanical Properties of a Model BisGMA/TEGDMA Composite Initially and after Storage." *Journal of Biomedical Materials Research-Part B Applied Biomaterials* 101 (8): 1469–76. https://doi.org/10.1002/jbm.b.32967.

Liu, Fengwei, Xiaoze Jiang, Qinghong Zhang, and Meifang Zhu. 2014. "Strong and Bioactive Dental Resin Composite Containing Poly(Bis-GMA) Grafted Hydroxyapatite Whiskers and Silica Nanoparticles." *Composites Science and Technology* 101: 86–93. https://doi.org/10.1016/j.compscitech.2014.07.001.

Liu, Fengwei, Bin Sun, Xiaoze Jiang, Sultan S. Aldeyab, Qinghong Zhang, and Meifang Zhu. 2014. "Mechanical Properties of Dental Resin/Composite Containing Urchin-like Hydroxyapatite." *Dental Materials* 30 (12): 1358–68. https://doi.org/10.1016/j.dental.2014.10.003.

Loumprinis, Nikolaos, Eva Maier, Renan Belli, Anselm Petschelt, George Eliades, and Ulrich Lohbauer. 2020. "Viscosity and Stickiness of Dental Resin Composites at Elevated Temperatures." *Dental Materials*. https://doi.org/10.1016/j.dental.2020.11.024.

Lung, Christie Ying Kei, and Jukka Pekka Matinlinna. 2012. "Aspects of Silane Coupling Agents and Surface Conditioning in Dentistry: An Overview." *Dental Materials* 28 (5): 467–77. https://doi.org/10.1016/j.dental.2012.02.009.

Matinlinna, Jukka Pekka, Christie Ying Kei Lung, and James Kit Hon Tsoi. 2018. "Silane Adhesion Mechanism in Dental Applications and Surface Treatments: A Review." *Dental Materials* 34 (1): 13–28. https://doi.org/10.1016/j.dental.2017.09.002.

McCabe, John F., and W.G. Angus Walls. 1969. *Applied Dental Materials. Br Stand Inst Br Stand*.

Miao, Xiaoli, Yaogang Li, Qinghong Zhang, Meifang Zhu, and Hongzhi Wang. 2012. "Low Shrinkage Light Curable Dental Nanocomposites Using SiO 2 Microspheres as Fillers." *Materials Science and Engineering C* 32 (7): 2115–21. https://doi.org/10.1016/j.msec.2012.05.053.

Miletic, Vesna. 2018. *Dental Composite Materials for Direct Restorations. Dental Composite Materials for Direct Restorations*.

Najafi, Hamed, Babak Akbari, Farhood Najafi, Amirbabak Abrishamkar, Arash Ramedani, and Abolfazl Yazdanpanah. 2017. "Evaluation of Relationship among Filler Amount, Degree of Conversion, and Cytotoxicity: Approaching Performance Enhancement Novel Design for Dental Bis-GMA/UDMA/TEGDMA Composite." *International Journal of Polymeric Materials and Polymeric Biomaterials* 66 (16): 844–52. https://doi.org/10.1080/00914037.2016.1277223.

Neuse, Eberhard, and Eliakim Mizrahi. 2003. "Bonding Materials and Techniques in Dentistry." In *Handbook of Adhesive Technology, Revised and Expanded*. CRC Press. https://doi.org/10.1201/9780203912225.ch49.

Plueddemann, Edwin P. 1991. *Silane Coupling Agents*. *Silane Coupling Agents*. Springer US. https://doi.org/10.1007/978-1-4899-2070-6.

Porto, Isabel Cristina Celerino de Moraes, Luis Eduardo Silva Soares, Airton Abrahão Martin, Vanessa Cavalli, and Priscila Christiane Suzy Liporoni. 2010. "Influence of the Photoinitiator System and Light Photoactivation Units on the Degree of Conversion of Dental Composites." *Brazilian Oral Research* 24 (4): 475–81. https://doi.org/10.1590/S1806-83242010000400017.

Pratap, Bhanu, Ravi Kant Gupta, Bhuvnesh Bhardwaj, and Meetu Nag. 2019. "Resin Based Restorative Dental Materials: Characteristics and Future Perspectives." *Japanese Dental Science Review* 55 (1): 126–38. https://doi.org/10.1016/j.jdsr.2019.09.004.

Rao, Tentu Nageswara, Imad Hussain, Ji Eun Lee, Akshay Kumar, and Bon Heun Koo. 2019. "Enhanced Thermal Properties of Zirconia Nanoparticles and Chitosan-Based Intumescent Flame Retardant Coatings." *Applied Sciences (Switzerland)* 9 (17). https://doi.org/10.3390/app9173464.

Razali, R. A.C., N. A. Rahim, I. Zainol, and A. M. Sharif. 2018. "Preparation of Dental Composite Using Hydroxyapatite from Natural Sources and Silica." In *Journal of Physics: Conference Series*. Vol. 1097. Institute of Physics Publishing. https://doi.org/10.1088/1742-6596/1097/1/012050.

Rueggeberg, Frederick Allen, Marcelo Giannini, Cesar Augusto Galvão Arrais, and Richard Bengt Thomas Price. 2017. "Light Curing in Dentistry and Clinical Implications: A Literature Review." *Brazilian Oral Research*. Sociedade Brasileira de Hematologia e Hemoterapia. https://doi.org/10.1590/1807-3107BOR-2017.vol31.0061.

Santini, Ario. 2010. "DentalMaterialScience Current Status of Visible Light Activation Units and the Curing of Light-Activated Resin-Based Composite Materials." *Dent Update*. Vol. 37.

Santini, Ario, Iranzihuatl Torres Gallegos, and Christopher M. Felix. 2013. "Photoinitiators in Dentistry: A Review." *Primary Dental Journal* 2 (4): 30–33. https://doi.org/10.1308/205016814809859563.

Santos, C, R L Clarke, M Braden, F Guitian, and K W M Davy. 2002. "Water Absorption Characteristics of Dental Composites Incorporating Hydroxyapatite Filler." *Biomaterials*. Vol. 23.

Shao, Gaofeng, Xiaodong Wu, Yong Kong, Sheng Cui, Xiaodong Shen, Chunrong Jiao, and Jian Jiao. 2015. "Thermal Shock Behavior and Infrared Radiation Property of Integrative Insulations Consisting of MoSi2/Borosilicate Glass Coating and Fibrous ZrO2 Ceramic Substrate." *Surface and Coatings Technology* 270 (May): 154–63. https://doi.org/10.1016/j.surfcoat.2015.03.008.

Sideridou, Irini D., and Maria M. Karabela. 2009. "Effect of the Amount of 3-Methacyloxypropyltrimethoxysilane Coupling Agent on Physical Properties of Dental Resin Nanocomposites." *Dental Materials* 25 (11): 1315–24. https://doi.org/10.1016/j.dental.2009.03.016.

Wang, Yazi, Hongfei Hua, Hongmei Liu, Meifang Zhu, and X. X. Zhu. 2020. "Surface Modification of ZrO2Nanoparticles and Its Effects on the Properties of Dental Resin Composites." *ACS Applied Bio Materials* 3 (8): 5300–5309. https://doi.org/10.1021/acsabm.0c00648.

Yushau, Umar S., Lama Almofeez, and Ayhan Bozkurt. 2020. "Novel Polymer Nanocomposites Comprising Triazole Functional Silica for Dental Application." *Silicon* 12 (1): 109–16. https://doi.org/10.1007/s12633-019-00104-w.

Zhang, Xiu Yin, Xin Jing Zhang, Zhuo Li Huang, Bang Shang Zhu, and R. R. Chen Rong-Rong. 2014. "Hybrid Effects of Zirconia Nanoparticles with Aluminum Borate Whiskers on Mechanical Properties of Denture Base Resin PMMA." *Dental Materials Journal* 33 (1): 141–46. https://doi.org/10.4012/dmj.2013-054.

Zhang, Ya Rong, Wen Du, Xue Dong Zhou, and Hai Yang Yu. 2014. "Review of Research on the Mechanical Properties of the Human Tooth." *International Journal of Oral Science*. Sichuan University Press. https://doi.org/10.1038/ijos.2014.21.

Zhou, Xinxuan, Xiaoyu Huang, Mingyun Li, Xian Peng, Suping Wang, Xuedong Zhou, and Lei Cheng. 2019. "Development and Status of Resin Composite as Dental Restorative Materials." *Journal of Applied Polymer Science* 136 (44): 1–12. https://doi.org/10.1002/app.48180.